Novel, improved grading system(s) for IDH-mutant astrocytic gliomas

Shirahata, Mitsuaki ; Ono, Takahiro ; Stichel, Damian ; et al ; Weller, Michael

Abstract: According to the 2016 World Health Organization Classification of Tumors of the Central Nervous System (2016 CNS WHO), IDH-mutant astrocytic gliomas comprised WHO grade II diffuse astrocytoma, IDH-mutant (AII), WHO grade III anaplastic astrocytoma, IDH-mutant (AAIII), and WHO grade IV glioblastoma, IDH-mutant (GBM). Notably, IDH gene status has been made the major criterion for classification while the manner of grading has remained unchanged: it is based on histological criteria that arose from studies which antedated knowledge of the importance of IDH status in diffuse astrocytic tumor prognostic assessment. Several studies have now demonstrated that the anticipated differences in survival between the newly defined AII and AAIII have lost their significance. In contrast, GBM still exhibits a significantly worse outcome than its lower grade IDH-mutant counterparts. To address the problem of establishing prognostically significant grading for IDH-mutant astrocytic gliomas in the IDH era, we undertook a comprehensive study that included assessment of histological and genetic approaches to prognosis in these tumors. A discovery cohort of 211 IDH-mutant astrocytic gliomas with an extended observation was subjected to histological review, image analysis, and DNA methylation studies. Tumor group-specific methylation profiles and copy number variation (CNV) profiles were established for all gliomas. Algorithms for automated CNV analysis were developed. All tumors exhibiting 1p/19q codeletion were excluded from the series. We developed algorithms for grading, based on molecular, morphological and clinical data. Performance of these algorithms was compared with that of WHO grading. Three independent cohorts of 108, 154 and 224 IDH-mutant astrocytic gliomas were used to validate this approach. In the discovery cohort several molecular and clinical parameters were of prognostic relevance. Most relevant for overall survival (OS) was CDKN2A/B homozygous deletion. Other parameters with major influence were necrosis and the total number of CNV. Proliferation as assessed by mitotic count, which is a key parameter in 2016 CNS WHO grading, was of only minor influence. Employing the parameters most relevant for OS in our discovery set, we developed two models for grading these tumors. These models performed significantly better than WHO grading in both the discovery and the validation sets. Our novel algorithms for grading IDH-mutant astrocytic gliomas overcome the challenges caused by introduction of IDH status into the WHO classification of diffuse astrocytic tumors. We propose that these revised approaches be used for grading of these tumors and incorporated into future WHO criteria.

DOI: https://doi.org/10.1007/s00401-018-1849-4

Shirahata, Mitsuaki; Ono, Takahiro; Stichel, Damian; et al; Weller, Michael (2018). Novel, improved grading system(s) for IDH-mutant astrocytic gliomas. Acta Neuropathologica, 136(1):153-166.
DOI: https://doi.org/10.1007/s00401-018-1849-4

Novel, improved grading system(s) for IDH-mutant astrocytic gliomas

Mitsuaki Shirahata [1,2,*], Takahiro Ono [1,3,*], Damian Stichel [4,*], Daniel Schrimpf [1,4], David E. Reuss [1,4], Felix Sahm [1,4], Christian Koelsche [1,4], Annika Wefers [1,4], Annekathrin Reinhardt [1,4], Kristin Huang [1,4], Philipp Sievers [1,4],Hiroaki Shimizu [3], Hiroshi Nanjo [5], Yusuke Kobayashi [2], Yuhei Miyake [2], Tomonari Suzuki [2], Jun-ichi Adachi [2], Kazuhiko Mishima [2], Atsushi Sasaki [6], Ryo Nishikawa [2], Melanie Bewerunge-Hudler [7], Marina Ryzhova [8], Oksana Absalyamova [8], Andrey Golanov [8], Peter Sinn [9], Michael Platten [10], Christine Jungk [11], Frank Winkler [12], Antje Wick [12], Daniel Hänggi [13], Andreas Unterberg [11], Stefan M. Pfister [14,15, 16], David T. W. Jones [14,15], Martin van den Bent [17], Monika Hegi [18], Pim French [17], Brigitta G. Baumert [19], Roger Stupp [20], Thierry Gorlia [21], Michael Weller [22], David Capper [23], Andrey Korshunov [1,4], Christel Herold-Mende [11], Wolfgang Wick [12], David N. Louis [24], Andreas von Deimling [1,4,]

[1] Department of Neuropathology, Institute of Pathology, Heidelberg University Hospital, Heidelberg, Germany
[2] Department of Neuro-Oncology/Neurosurgery, Saitama Medical University International Medical Center, Hidaka, Japan
[3] Department of Neurosurgery, Akita University Graduate School of Medicine, Akita, Japan
[4] Clinical Cooperation Unit Neuropathology, German Cancer Consortium (DKTK), German Cancer Research Center (DKFZ) Heidelberg, Germany
[5] Akita University Hospital Division of Clinical Pathology, Akita, Japan
Medical Center, Hidaka, Japan
[6] Department of Pathology, Saitama Medical University International Medical Center, Hidaka, Japan
[7] Genomics and Proteomics Core Facility, German Cancer Research Center (DKFZ), Heidelberg, Germany
[8] NN Burdenko Neurosurgical Institute, 5-th Tverskaya_Yamskaya str. 16 Moscow, Russia
[9] Department of Pathology, University Hospital Heidelberg, Heidelberg, Germany
[10] Department of Neurology, Universitätsmedizin Mannheim, Medical Faculty Mannheim, Heidelberg University, Mannheim, Germany
[11] Department of Neurosurgery, Heidelberg University Hospital, Heidelberg, Germany
[12] Department of Neurology, Heidelberg University Hospital, Heidelberg, and Clinical Cooperation Unit Neurooncology, German Cancer Consortium (DKTK), German Cancer Research Center (DKFZ) Heidelberg, Germany
[13] Department of Neurosurgery, University Medical Center Mannheim, University of Heidelberg
[14] Hopp Children´s Cancer Center at the NCT Heidelberg (KiTZ)

[15] Division of Pediatric Neurooncology, German Cancer Consortium (DKTK), German Cancer Research Center (DKFZ), Heidelberg, Germany
[16] Department of Pediatric Oncology, Hematology and Immunology, University Hospital Heidelberg, Heidelberg, Germany
[17] The Brain Tumor Center at Erasmus MC Cancer Institute, Rotterdam, The Netherlands
[18] Laboratory of Brain Tumor Biology and Genetics, Neuroscience Research Center, Lausanne University Hospital, Lausanne, and Division of Neurosurgery, Lausanne University Hospital, Lausanne, Switzerland
[19] Department of Radiation-Oncology (MAASTRO Clinic) & GROW (School for Oncology), Maastricht University Medical Centre, Maastricht, The Netherlands
[20] Malnati Brain Tumor Institute of the Lurie Cancer Center, Northwestern University Feinberg School of Medicine, Chicago, IL, USA
[21] EORTC Headquarter, Brussels, Belgium
[22] Department of Neurology, University Hospital and University of Zurich, Zurich, Switzerland
[23] Department of Neuropathology, University Hospital Heidelberg, ,and German Cancer Consortium (DKTK), Partner Site Berlin, German Cancer Research Center (DKFZ) Heidelberg,and Charité – Universitätsmedizin Berlin, corporate member of Freie Universität Berlin, Humboldt-Universität zu Berlin, and Berlin Institute of Health, Department of Neuropathology
[24] Department of Pathology, Massachusetts General Hospital and Harvard Medical School, Boston, MA 02114, USA
* The first three authors have contributed equally

Corresponding author
Andreas von Deimling
Department for Neuropathology and CCU Neuropathology
University of Heidelberg and DKFZ
Im Neuenheimer Feld 224
69120 Heidelberg
Fon: +49-6221-56 4650
Fax: +49-6221-56 4566
andreas.vondeimling@med.uni-heidelberg.de

Summary

According to the 2016 World Health Organization Classification of Tumors of the Central Nervous System (2016 CNS WHO), IDH-mutant astrocytic gliomas are comprised of WHO grade II diffuse astrocytoma, IDH-mutant (AII_{IDHmut}), WHO grade III anaplastic astrocytoma, IDH-mutant ($AAIII_{IDHmut}$), and WHO grade IV glioblastoma, IDH-mutant (GBM_{IDHmut}). Notably, IDH gene status has been made the major criterion for classification while the manner of grading has remained unchanged: it is based on histological criteria that arose from studies which antedated knowledge of the importance of IDH status in diffuse astrocytic tumor prognostic assessment. Several studies have now demonstrated that the anticipated differences in survival between the newly defined AII_{IDHmut} and $AAIII_{IDHmut}$ have lost their significance. In contrast, GBM_{IDHmut} still exhibits a significantly worse outcome than its lower grade IDH-mutant counterparts. To address the problem of establishing prognostically significant grading for IDH-mutant astrocytic gliomas in the IDH era, we undertook a comprehensive study that included assessment of histological and genetic approaches to prognosis in these tumors. A discovery cohort of 211 IDH-mutant astrocytic gliomas with an extended observation was subjected to histological review, image analysis, and DNA methylation studies. Tumor group–specific methylation profiles and copy number variation profiles (CNV) were established for all gliomas. Algorithms for automated CNV analysis were developed. All tumors exhibiting 1p/19q codeletion were excluded from the series. We developed algorithms for grading, based on molecular, morphological and clinical data. Performance of these algorithms was compared with that of WHO grading. Three independent cohorts of 108, 154 and 224 IDH-mutant astrocytic gliomas were used to validate this approach. In the discovery cohort several molecular and clinical parameters were of prognostic relevance. Most relevant for overall survival (OS) was *CDKN2A/B* homozygous deletion. Other parameters with major influence were necrosis and the total number of CNV. Proliferation as assessed by mitotic count, which is a key parameter in 2016 CNS WHO grading, was of only minor influence. Employing the parameters most relevant for OS in our discovery set, we developed two models for grading these tumors. These models performed significantly better than WHO grading in both the discovery and the validation sets. Our novel algorithms for grading IDH-mutant astrocytic gliomas overcome the challenges caused by introduction of IDH status into the WHO classification of diffuse astrocytic tumors. We propose that these revised approaches be used for grading of these tumors and incorporated into future WHO criteria.

Keywords:
Astrocytoma, Glioblastoma, IDH, grading, CDKN2A/B

Introduction

Diffuse astrocytic gliomas are the most common brain tumors of adults and their grading has therefore been of considerable significance in the management of patients with brain tumors. As a result, over the years, these tumors have been graded according to various systems, each representing an advance over prior approaches. These have included the Kernohan scheme, the St. Anne-Mayo system and, for the past 25 years, primarily the WHO classification [8,12,13]. These schemes often resulted in patient groups with significantly varying prognoses that received treatments of differing intensity. In recent years the WHO classification scheme based on early work from Zulch [38] and regarding astrocytic gliomas from Burger [3] has been most widely used [13,14].

IDH1 and *IDH2* mutations have emerged as early mutations in diffuse astrocytic tumors [2,21,35,37], and determination of the IDH status by immunohistochemistry [6] or sequencing has now become a standard in the diagnosis of these tumors. The 2016 WHO Classification Of Tumors Of The Central Nervous System [14] introduced molecular parameters for the categorization of diffuse astrocytomas, notably *IDH* mutation status [14]. In fact, determination of *IDH* and 1p/19q status is mandatory for diagnosing beyond NOS (not otherwise specified) categories. However, applying the new classification parameters results in patient groups that are different from those classified prior to the 2016 CNS WHO (e.g. according to the 2007 CNS WHO). From the former group of diffuse WHO grade II and III astrocytomas, approximately 70% to 80% now are classified as diffuse astrocytoma, IDH-mutant (AII_{IDHmut}) and anaplastic astrocytoma, IDH-mutant ($AAIII_{IDHmut}$) while 20% to 30% are classified as diffuse astrocytoma, IDH-wildtype (AII_{IDHwt}) and anaplastic astrocytoma, IDH-wildtype ($AAIII_{IDHwt}$). In turn, the shifting of diagnostic groups has prognostic implications. For example, multiple studies have demonstrated a close relationship between many AII_{IDHwt}/$AAIII_{IDHwt}$ to glioblastoma, IDH-wildtype (GBM_{IDHwt}) [4,27,33]. In fact, prior to the 2016 CNS WHO the prognostic power of grading parameters for diffuse astrocytoma WHO grade II (AII_{NOS}) and anaplastic astrocytoma WHO grade III ($AAIII_{NOS}$) were most likely a result of considerable contamination with unrecognized GBM_{IDHwt} [34]. In addition, a series of recent studies have highlighted that WHO grading of AII_{IDHmut}/$AAIII_{IDHmut}$ has lost its prognostic relevance [4,18,20,22,28,33,34]. Given the clinical importance of appropriate grading, the potential prognostic changes brought about by the 2016 CNS WHO classification pose a major challenge. We therefore sought to establish novel, improved grading criteria for IDH-mutant astrocytic gliomas.

Methods

Study design and participants

For this multicenter retrospective analysis we collected a discovery series of 211 astrocytic tumors. We defined the following criteria for inclusion: 1) all tumors had either an *IDH1* or an *IDH2* mutation; 2) all tumors had a 2016 CNS WHO integrated diagnosis of AII_{IDHmut} (n=54), $AAIII_{IDHmut}$ (n=90) or GBM_{IDHmut} (n=67), i.e., no tumors had 1p/19q codeletion; 3) sufficient formalin-fixed, paraffin-embedded (FFPE) material for morphological and additional molecular analyses was available; and 4) the patients had an extended follow up. Tumor material was from the archive of the Department of Neuropathology, University of Heidelberg, Heidelberg, Germany and from patients enrolled in the NOA04 trial [36]. Use of tissue and clinical data was in accordance with local ethical regulations.

Three validation series were compiled. The first validation series from Heidelberg (HD) containing 108 tumors differed from the discovery set only in that sufficient material for the complete set of analyses performed on the discovery set was not available. The HD validation series contained AII_{IDHmut} (n=32), $AAIII_{IDHmut}$ (n=29) and GBM_{IDHmut} (n=47). In this set diagnosis and grading according to the guidelines of the 2016 CNS WHO was performed (AvD). The second validation set from the European Organization for Research and Treatment of Cancer (EORTC) contained 154 cases and was compiled from patients of the EORTC studies 22033 (64 cases), 26091 (80 cases) and 26981 (10 cases) with Illumina 450k or 850k/EPIC data being available. All patients in this set also had an IDH mutation and none of the tumors harbored a 1p/19q codeletion. The EORTC validation series contained AII_{IDHmut} (n=94), $AAIII_{IDHmut}$ (n=39) and GBM_{IDHmut} (n=21). In this set diagnosis and grading according to the guidelines of the 2016 CNS WHO was performed by reference centers. The third validation set from The Cancer Genome Atlas consortium (TCGA) contained 224 cases and was retrieved from published data. In this set diagnosis and grading was obtained from the source. Methylome data based on Illumina 450k array was available for all of these cases. All cases in this set had an IDH mutation as provided by TCGA. and none contained a 1p/19q codeletion as assessed by copy number profiles which were calculated from the DNA methylation data. Clinical data were known to the local investigators (MS, TO, DSt, DSc, AvD). Cases from the HD validation set also were reviewed by the same neuropathologist (AvD). Clinical data from the HD validation set were known to the lead authors. Clinical data from the EORTC validation set were not known to the lead authors. Clinical data for the TCGA validation set were open access. The institutional funding of this study did not influence study design, inclusion criteria, analyses or interpretation of the data. MS, TO, DSt,

DSc and AvD had full access to all raw data except for the EORTC series and had final responsibility for the decision to submit for publication.

Procedures

For the discovery set, 4µm-sections were cut from FFPE blocks from all tumors and stained with hematoxylin/eosin, and examined by immunohistochemistry with antibodies against IDHR132H (clone H09, Dianova, Hamburg, Germany), Ki-67 (clone MIB-1, Dako, Waldbronn, Germany) or pHH3 (rabbit polyclonal,BioCare Medical, Pacheco, USA) to determine proliferation and CD31 (clone JC70A, Dako, Waldbronn, Germany) to determine vascular density.

All tumor samples were analyzed by Illumina HumanMethylation450 (450k) or MethylationEPIC (850k) arrays (Illumina, San Diego, CA, USA) as previously described [32]. Methylation data were analyzed by a classifier as previously reported [5]. CNV plots were generated using the R/Bioconductor package conumee version 1.6.0. Automated assessment of copy-number changes was performed using a proprietary algorithm (Stichel D and colleagues, unpublished). This allowed determining CNV load (CNV-L) for each tumor.

The discovery set was subjected to digital image analysis. Parameters assessed included cell count, proliferation activity and microvessel density. The software package Aperio ImageScope was employed for proliferation and microvessel density analysis. The software packages Ilastik [31] and ImageJ [30] were used for cell count analysis. To receive subgroups with distinct OS, conditional trees were created applying the function ctree from the R package party on the discovery set and a set of selected input variables. Here, the global null hypothesis of independence between any of the input variables and the OS was tested. If it couldn't be rejected, the association of any single input variable with the response was computed as p-value from a test for the partial null hypothesis of the variable and OS. The input variable with the highest association to OS was selected and a binary split in this variable was created. This procedure was then repeated to create conditional trees. To create $Model_{path}$ all parameters received from molecular analyses but CDKN2A/B status were excluded. Kaplan-Meier estimators were computed using the function survfit from the R package survival. All parameters assessed are listed in table 1.

Numerical alterations of several genes with established relevance for astrocytic gliomas--comprising *CCND1*, *CCND2*, *CDK4*, *CDK6*, *CDKN2A/B*, *EGFR*, *MDM4*, *MET*, *MYC*, *MYCN*, *NF1*, *NF2*, *PDGFR2*, *PPM1D*, *PTEN*, *RB1* and *SMARCB1*-- were evaluated by visual assessment of copy number profiles and by employing our proprietary algorithm. Our series are based on visual assessment for *CDKN2A/B* analysis. With the cutoff selected in our series, visual and algorithm driven *CDKN2A/B* evaluation produced the same number of cases scored as having a homozygous deletion. The respective genes and cutoff values are given in table 2.

Statistical analysis

All patient sets were retrospectively compiled. The size of the respective sets was determined by availability of data and not by a power calculation. OS times were analyzed by the Kaplan-Meier method and compared with a log-rank test. Prediction error plots were based on Brier scores. P values less than 0.05 were considered significant. Software R version 3.4 and packages survival and party were employed for analysis

Results

Series validation and determination of histologic and molecular features associated with OS

On the basis of histological review, all tumors in the discovery set were confirmed to be diffuse astrocytic gliomas. Classification according to the 2016 CNS WHO revealed three distinct groups, AII_{IDHmut}, $AAIII_{IDHmut}$ or GBM_{IDHmut}, with significantly different OS (figure 1a). The IDH status was determined by IHC with H09 [6] or by Sanger sequencing. All immunonegative samples have been subjected to sequencing. IDH status was also confirmed by performing 450k/EPIC analysis and receiving the readout of “methylation group astrocytoma IDH mutant” by a recently developed and published classifier tool [5] which predicts IDH-mutant astrocytoma with very high specificity and sensitivity. Further, combined 1p/19q deletion was excluded for every tumor based on analysis of the copy number profile (CNP) generated from 450k/EPIC data. Therefore, our series included exclusively $AII_{IDHmut,}$ $AAIII_{IDHmut}$ or $GBM_{IDHmut,}$ in full agreement with 2016 CNS WHO classification criteria. In the discovery set of 211 patients, 135 were still alive at the time of last follow-up. Median follow up in these 135 patients was 1772 days (4.9 years); average follow was 2086 days (5.7 years).

The morphological parameters of strongest negative prognostic value were vascular proliferation ($p<0.0005$) and necrosis ($p<0.00005$). Patients aged 55 and older did worse ($p<0.04$) than patients aged below this cutoff confirming the influence of age on OS. Female patients fared significantly ($p=0.01$) better than male patients. Image analysis showed that cellularity had a major association with OS. Cell count defined as number of tumor cells per square millimeter in the tumor area of highest density emerged as an important parameter for prognostic evaluation. Patients with a cell density of 4605/mm^2 or more fared worse than patients with 4604 or fewer tumor cells/mm^2 ($p<0.002$) Ki-67 immunohistochemistry was significantly associated with worse OS (cutoff 14.5%; $p<0.006$), however, mitotic count established by assessing sections treated with pHH3 antibody was not prognostic. (table 1). While pHH3 has been established as a reliable marker for assessing mitotic activity, those studies have mainly been performed prior to further stratification of diffuse astrocytomas by IDH status [7]. In a recent study on *IDH*-mutant diffuse glioma, pHH3 was found to reliably detect mitotic figures but turned out with a weaker association with survival that Ki-67 [10].

EPIC- or 450k array data were employed to assess several parameters: this included analysis by the brain tumor classifier tool [5] for the confirmation of *IDH* mutations and evaluation of individual copy number status. Copy number plots were evaluated for amplifications or homozygous deletions, respectively. In the discovery set regions with such alterations contained *CCND1*, *CCND2*, *CDK4*, *CDK6*, *CDKN2A/B*, *EGFR*, *MDM4*, *MET*,

MYC, *MYCN*, *NF1*, *NF2*, *PDGFR2*, *PPM1D*, *PTEN*, *RB1* and *SMARCB1* (table 2). Upon univariate analysis the strongest association with OS was observed for homozygous *CDKN2A*/B deletion and for *MYCN* amplification (table 2 and figure 1b). Furthermore, the total CNV-load (CNVL) was determined, resulting in a split for a value of 349695798 base pairs (rounded 350 Mb). This number refers to the sum of all gains or deletions as determined by analysis of the 450k/850k raw data by our proprietary algorithm.
Patients with higher CNVL fared significantly worse than patients with lower CNVL ($p<0.0001$). However the frequency for all chromosomal gains or losses increased with age as demonstrated by summary CNV plots (supplementary figure 1). Further, EPIC/450k array methylation data were used for unsupervised clustering of the discovery dataset. This analysis yielded two sets with highly significant differences in OS (supplementary figure 2A). Likewise, the algorithm underlying our methylation based classifier [5] recognized two sets with significantly different OS (supplementary figure 2D).

Novel grading algorithms based on discovery set

Multivariate analysis including all parameters exhibiting a significant association with OS (table 1) was performed to develop grading models that could be compared with the current 2016 CNS WHO standard. Three different models were generated. The first approach ($Model_{path}$) aimed at minimizing the required molecular data input, which would presumably allow for the most widespread applicability. In addition to IDH and 1p/19q testing, the first approach only requires the determination of *CDKN2A/B* status. The second approach, $Model_{CNVL}$ made use of all molecular data available. Because $Model_{CNVL}$ in the discovery set placed a set of 7 patients with necrosis into the most favorable group, we created a $Model_{combined}$, which shifted these patients to the patient group with intermediate OS (Figure 2). While this model was not based on a mathematical procedure, it worked well in the discovery and all validation sets.
$Model_{path}$ demonstrated that an algorithm based on employment of absence/presence of homozygous *CDKN2A/B* deletion and absence/presence of necrosis formed three groups among the 211 tumors in the discovery cohort. In this $Model_{path}$, patients with homozygous deletion of *CDKN2A/B* exhibited the worst OS and were termed astrocytoma, IDH-mutant, grade 4, pathology ($A4_{path}$). This group comprised 38 tumors of the discovery cohort and contained 23 GBM_{IDHmut} and 15 $AAIII_{IDHm}$. Tumors with necrosis but without homozygous *CDKN2A/B* deletion fared significantly better and were termed astrocytoma, IDH-mutant, grade 3, pathology ($A3_{path}$). $A3_{path}$ contained 44 tumors which by definition were all GBM_{IDHm}. The remaining 129 patients with neither homozygous *CDKN2A/B* deletion nor necrosis were termed astrocytoma, IDH-mutant, grade 2, pathology ($A2_{path}$). $A2_{path}$ contained 75 $AAIII_{IDHmut}$ and 54 AII_{IDHm}. OS plots of the discovery set assembled according to 2016 CNS WHO and

according to $Model_{path}$ are shown (figure 3a and 3b). $Model_{path}$ performed better in predicting OS of the groups than the 2016 CNS WHO did as illustrated by Brier scores (figure 4a). $Model_{CNVL}$ relied on absence/presence of homozygous *CDKN2A/B* deletion and on a threshold value of 350 Mb for CNVL. Therefore, A4 were determined as in our first approach. However, the remaining patients were subdivided with those having a CNV-L value < 350 Mb being termed astrocytoma, IDH-mutant, grade 2, CNVL ($A2_{CNVL}$) and those with value > 350 Mb being termed astrocytoma, IDH-mutant, grade 3, CNVL ($A3_{CNVL}$). $A2_{CNVL}$ featured 86 patients containing 7 $GBM_{IDHmut,}$ 42 $AAIII_{IDHmut}$ and 37 AII_{IDHm}. $A3_{CNVL}$ contained 87 patients, with 37 $GBM_{IDHmut,}$ 33 $AAIII_{IDHmut}$ and 17 AII_{IDHm}. A OS plot of the discovery set according to $Model_{CNVL}$ is shown (figure 3c). $Model_{CNVL}$ performed better in predicting OS of the groups than the 2016 CNS WHO did as illustrated by Brier scores (figure 4a).
$Model_{combined}$ was devised to circumvent the provocative shift of patients with necrosis but without *CDKN2A/B* deletion and with a low CNVL into the most favorable patient group (figure 2). Instead, this patient group was placed in the intermediate malignancy group. Notably, $Model_{combined}$ is not based on a strict mathematical approach. The number of only seven patients in this group is too small to confirm OS comparable to that of patients in the intermediate malignancy group (supplementary figure 3). In $Model_{combined}$ the A4 group defined by homozygous *CDKN2A/B* deletion was identical to that in $Model_{path}$ and $Model_{CNVL}$. $Model_{combined}$ also performed better in predicting OS of the groups than the 2016 CNS WHO could accomplish as illustrated by Brier scores (figure 4a).
Importantly, all three-tiered grading approaches, i.e. WHO, $Model_{path}$, $Model_{CNVL}$ and $Model_{combined}$ were predictive with higher power than two-tiered approaches based on unsupervised clustering and the classifier tool (figure 4a).

Validation of the study series

The validation sets supported our findings from the discovery set.
In the HD validation set, WHO based separation was of borderline significance (p=0.05) (Figure 3e). In contrast, $Model_{path}$ or $Model_{CNVL}$ both significantly separated three prognostic patient groups (p<0.0001) (figure 3f and g). Best performance was achieved by $Model_{combined}$ (Figure 3h).
The EORTC validation set produced comparable results (figure 3i, j, k, and l). Here the 2016 CNS WHO did separate groups with different OS (p=0.004). $Model_{path}$ performed slightly better (p=0.002), however, $Model_{CNVL}$ and $Model_{combined}$ again provided best separation into groups of different OS (p< 0.0001).
The TCGA dataset was only of limited value for validating our models due to a high number of cases with relatively short observation periods. We observed a good separation of patients recognized by our models as highly malignant due to presence of a homozygous *CDKN2A/B*

deletion. TCGA patients with *CDKN2A/B* homozygous deletion also died relatively quickly and therefore separated significantly from patients without such deletion. However, the separation between the intermediate and more favorable tumor groups was not possible due to a high number of patients lacking long-term follow up. Thus, due to its composition the TCGA validation set only could be used for validating the poor OS of patients with homozygous *CDKN2A/B* deletion (Figure 3m, n, o and p).

In conclusion, in all three validation sets the tested grading models performed better than the current WHO system.

Discussion

Using combined histological and genetic parameters, notably necrosis and *CDKN2A/B* deletion, we have established a novel grading system for IDH-mutant diffuse astrocytic tumors. Interestingly, this system does not incorporate morphological estimates of proliferation, which have been a key parameter in WHO grading systems through counting mitotic figures. Indeed, *CDKN2A/B* homozygous deletion is tightly linked to proliferation because loss of p16 removes the inhibition of complexes of CDK4 with D-type cyclins thereby driving the cell cycle. In our discovery set CDKN2A/B homozygous deletion was clearly associated with higher proliferation. However, a considerable fraction of patients lacking the deletion still exhibited high Ki-67 reads (supplementary figure 4).

By focusing on this marker rather than quantifying proliferation, grading accuracy may improve because the difficulties underlying precise determination of mitotic counts (e.g., interobserver variations, tissue artifacts, interfering staining conditions, sampling, or extended time from tissue removal to fixation) are eliminated.

In our discovery set, mitotic count was not a strong predictor of outcome. This confirms previous reports pointing to the failure of morphological proliferation assessment in predicting clinical outcome in IDH-mutant astrocytic gliomas [20,28]. Likewise, Ki67 staining ubiquitously used as a parameter for estimating proliferation provides variable readouts dependent on staining or processing conditions and, therefore, is problematic for the determination of cutoff values to discern malignancy grades.

Proliferation assessed by Ki-67 is described as low or absent in AII_{IDHmut} in the 2016 CNS WHO 2016 [17]. In our discovery set, Ki-67 is significantly associated prognosis, but the split point was determined around 15%. A reason for the failure of Ki-67 as a prognostic parameter in WHO is the low split point (often near 2%) in the previous studies [11,15]. These studies all were from the pre-IDH era and contained many glioblastomas, thus driving the split points to low values. This may explain why the 2016 CNS WHO stated that Ki-67 was not prognostic for $AAIII_{IDHmut}$ [17].

The presence of homozygous *CDKN2A/B* deletion turned out to be the most powerful parameter for inferior clinical outcome. This parameter is currently not employed in WHO grading, but could be construed as a molecular estimate of proliferation given the role of the p16 protein in regulating the cell cycle. Interestingly, *CDKN2A/B* homozygous deletion in tumors without necrosis, graded $AAIII_{IDHmut,}$ was associated with OS indistinguishable from that of patients with tumors exhibiting both *CDKN2A/B* homozygous deletion and necrosis that were diagnosed by definition as GBM_{IDHmut} (figure 1b). And in turn, by removing tumors with *CDKN2A/B* homozygous deletion among $AAIII_{IDHmut,}$ OS of the remaining patients did not significantly ($p = 0.124$) differ from that AII_{IDHmut} (figure 1b). *CDKN2A/B* homozygous

deletion or mutations in the RB pathway have been determined as an unfavorable parameter in previous studies [1,26]. We therefore performed an analysis combining cases with either *CDKN2A/B* homozygous deletion or *RB1* homozygous deletion or *CDK4* or *CDK6* amplification. However, this did not result in an overall improvement of separating groups of patients with different outcome in all tumor sets. We think this partly due to the more pronounced association of *CDKN2A/B* homozygous deletion with survival than that of the other RB1 pathway genes analyzed (supplementary figure 5) While combining typical lesions of the RB1 pathway should be further explored, we expect that mainly the assessment of *CDKN2A/B* status will be highly relevant for future diffuse astrocytoma grading systems. Satisfactory data acquisition can be performed by FISH, by quantitative PCR or by array technology as performed in this study. As shown elsewhere, *CDKN2A/B* status may be readily determined by FISH analysis [23,25]. Given the utility of immunohistochemistry for routine pathology diagnosis, we tried to detect homozygous deletion of the *CDKN2A* gene product p16 by immunohistochemistry. Unfortunately, using p16 antibody cloneG175-405 (BD-Biosciences) we could not show satisfactory correlation between p16 immunohistochemistry and molecular detection of *CDKN2A* homozygous deletion. In our immunohistochemistry, the basal nuclear expression of p16 was too low in many samples to allow definite detection of loss of expression. Our observation is supported by another study observing a correlation of p16 expression loss and *CDKN2A* deletion, however only in 85% of the deleted tumors [25]. We consider this correlation not tight enough and, therefore, favor determination of *CDKN2A/B* deletion by an assay addressing DNA directly. A representative CNP with evident *CDKN2A/B* homozygous deletion is shown in supplementary figure 6. Another key parameter, the presence of necrosis, which according to the 2016 CNS WHO results in the diagnosis of $GBM_{IDHmut,}$ appears overrated in terms of estimating prognosis in IDH-mutant diffuse astrocytomas. As a single factor, necrosis is prognostically highly significant in our discovery set (table1), but the presence of necrosis in the absence of homozygous *CDKN2A/B* deletion was associated with clearly better prognosis than that of tumors containing the homozygous deletion (figure 1b). To account for these observations, we developed grading models based on those parameters that turned out to predict clinical outcome better than grading according to the 2016 CNS WHO (figure 2). Better outcome prediction could be confirmed in two independent validation series and better detection of patients at risk for poor OS could be achieved in the TCGA set with shorter observation periods only (figure 3). Our data on the TCGA data are in line with a previous study on the TCGA LGG data set reporting that CDKN2A homozygous deletion, but not expression associates with unfavorable OS [29]. Because all three tiered grading approaches in this study predicted OS with less error than the two-tiered grading schemes emerging from unsupervised clustering or from using the methylation-based classifier [5], the latter were not

further considered, although both schemes proved stable in the validation series (figure 4a and b and supplementary figure 2a, b, c, d, e ,f and 5)
An interesting parameter emerging from our analysis was CNVL. A proportion higher than 350 Mb either lost or gained in the areas covered by the methylation arrays correlated with poorer OS. Previously, the mutational load has been shown to correlate with tumor grade in IDH-mutant glioma [9]. While our data more reflect genomic instability and those data rely on an accumulation of mutations they also support a quantitative approach to tumor grading.

Shifts of patients according to different grading approaches

WHO grading and our grading models result in three different groups, however with different distributions. The allotment of patients in the discovery set to Model-specific sets is provided in supplementary table 1. Our novel approaches lead to a higher overall number of diffuse astrocytomas in the lower-grade group. This effect is more pronounced for $Model_{path}$ than for $Model_{CNVL}$. In $Model_{path}$, the increase from 54 AII_{IDHmut} to 129 $A2_{path}$ comes with the reduction of median OS from 7053 days to 5122 days. In contrast, the increase from 54 AII_{IDHmut} to 86 $A2_{CNVL}$ did not alter the median OS of 7053 days. The shifts in patient numbers in the comparable groups is mainly due to the strong influence of proliferation rate on the WHO grading algorithm. The typical problem is exemplified by a well differentiated diffuse astrocytoma being currently diagnosed as a WHO grade III tumor because of the detection of a few mitotic figures. In such a setting, the clinician may be surprised by a grade III designation given the lack of neuroradiological or intraoperative evidence for higher grade. The novel grading approaches described here appear to address this clinicopathological problem. It should be noted that the diagnostic considerations underlying WHO grading of the discovery set already deviated from the traditional WHO guidelines due to the experience of the authors who diagnosed and graded the tumors [20,28] In particular, more than single mitoses were accepted as compatible with AII_{IDHmut}. In the setting of IDH mutations, the presence of few mitotic figures did not result in a diagnosis of $AAIII_{IDHmut}$. This may be another reason for “standard” grading successfully predicting OS in the discovery set.
Our data demonstrate that $AAIII_{IDHmut}$ stratified for *CDKNA* homozygous deletion separates into two groups with quite different OS: patients with tumors lacking this lesion follow a moderately aggressive course while patients with tumors having a *CDKN2A/B* deletion fare more similar to patients with GBM_{IDHmut} with homozygous deletion but much worse than patients with GBM_{IDHmut} lacking *CDKN2A/B* homozygous deletion (figure 1B). Thus combining patients with AII_{IDHmut} and $AAIII_{IDHmut}$ but lacking homozygous deletion of *CDKN2A/B* into a single group in $Model_{Path}$ forms a fairly homogenous cohort and may have implications for the nomenclature of these tumors as well as a potential therapeutic relevance.

$Model_{Path}$ results in reduction of the size of the intermediate grading group. In the discovery set, $AAIII_{IDHmut}$ with 90 patients constitutes the largest group. The equivalent group according to $Model_{path}$ includes 44 patients. This contrasts $Model_{CNVL}$ which allots 87 patients to the intermediate group. The relation of the A3path and A3CNVL groups is analyzed in $Model_{combined}$ based on *CDKN2A/B*, necrosis and CNV-L (figure 3b, c and d). The power of this model is best exemplified by the lowest prediction error rate as shown by Brier score (figure 4a for discovery set, figure 4b for HD-validation set).

Implication for the use of morphological parameters proliferation and necrosis

Our data challenge the value of two main criteria that have long been used in the grading of diffuse astrocytomas: proliferation and necrosis. As previously reported [20], mitotic count is of less significance in a set of IDH-mutant diffuse astrocytomas than in a set of diffuse astrocytomas not tested for IDH status (and thereby likely to contain a substantial fraction of biological glioblastomas). In our analyses, mitotic figures did not emerge as a parameter providing the most significant separation of patients with IDH-mutant diffuse astrocytoma in groups with different OS. We therefore suggest a more conservative use of proliferation and caution to use this as a sole indicator for high tumor grade.

The other grading parameter in question is necrosis. The presence of necrosis in a diffuse astrocytic neoplasm that had not been pretreated inevitably prompted the WHO diagnosis of GBM_{IDHmut}. However, patients with tumors exhibiting necrosis but not containing homozygous *CDKN2A/B* deletion survive significantly better than patients with tumors lacking necrosis but containing a *CDKN2A/B* homozygous deletion (figure 1b). This observation in our discovery and validation series (figure 3) should prompt a more conditional approach to the presence of necrosis as a parameter for grading of higher-grade diffuse astrocytic tumors.

Clinical perspective of grading according to the novel approaches

Caveats of our study are the heterogeneity of treatment and the potential effect of treatment on OS. Patients with $AAIII_{IDHmut}$ and $AII_{IDHmut.}$ have been treated quite heterogeneously with therapies ranging from wait and see to radiotherapy, chemotherapy or combinations thereof. In general, patients with $AAIII_{IDHmut}$ may have been likely to receive a more intense treatment than patients with AII_{IDHmut} .We cannot exclude the possibility of treatment being effective in patients with $AAIII_{IDHmut}$, thereby blurring the distinction to OS of patients with $AII_{IDHmut.}$. Nonetheless, the current treatment for AII_{IDHmut} and $AAIII_{IDHmut}$ is similar in most centers. Therefore, the shift of patients between the corresponding groups following grading according to our novel approaches will likely not have an immediate effect on treatment. However, upon applying $Model_{combined}$ we subdivide AII_{IDHmut} into $A2_{combined}$ and $A3_{combined}$. Patients with $A2_{combined}$, although more numerous than those in $AII_{IDHmut,}$ appear to exhibit a

slightly better OS than patients with AII_{IDHmut}. This may prompt future consideration regarding therapy in $A2_{combined}$ patients. In contrast, patients with $A3_{combined}$ show average OS closer to $AAIII_{IDHmut}$ patients, thereby potentially supporting similar treatments for these groups. In turn, it will be of interest to determine if patients with GBM_{IDHmut} should receive the same treatment as those patients with GBM_{IDHmut} lacking homozygous *CDKN2A/B* deletion since these patients have OS approaching that of $AAIII_{IDHmut}$. Finally, patients assigned to the least favorable A4 group all exhibit homozygous*CDKN2A/B* deletion; such patients are in need of maximal treatment and could possibly benefit from treatment with CDK antagonists because *CDKN2A/B* deletion results in increased CDK activity [24].

Implications for the classification and grading of IDH-mutant diffuse astrocytic tumors

The 2016 CNS WHO divided the traditionally termed "glioblastoma" into GBM_{IDHwt}, GBM_{IDHmut} and, in specific situations, diffuse midline glioma, *H3*K27–mutant. Genetically, these three groups are entirely different. While the diffuse midline glioma, *H3*K27–mutant is semantically clearly set apart from GBM_{IDHwt}, the latter shares the same "family name" with GBM_{IDHmut} [18]. However, there appears to be greater genetic kinship between GBM_{IDHmut} and A_{IDHmut} and not between GBM_{IDHmut} and GBM_{IDHwt}. This kinship is also supported by the distribution of other mutations such as *ATRX* or *TP53* that are typically seen in these tumors and by the rarity of many mutations typical for GBM_{IDHwt} such as *EGFR* amplification. Thus a genetic approach to taxonomy would favor a term such as "high-grade A_{IDHmut}" rather than the current term of GBM_{IDHmut}.

However, this still would be in conflict with a harmonious grading scale. Clearly, GBM_{IDHmut} has a better prognosis than GBM_{IDHwt}. In fact, GBM_{IDHmut} has a better prognosis than the prognosis allotted to the pre-IDH era anaplastic astrocytoma WHO grade III ($AAIII_{NOS}$) [34]. This circumstance would argue for a lower grade than currently allotted to the GBM_{IDHmut}. However, the novel creation of an IDH-mutant glioblastoma grade 3 would seem awkward[18].

We suggest that future grading approaches include assessment of homozygous *CDKN2A/B* deletion in these tumors, given its powerful association with poorer prognosis. This accounts for both GBM_{IDHmut} and $AAIII_{IDHmut}$ – resulting in essential irrelevance of the presence of necrosis on OS in tumors with homozygous *CDKN2A/B* deletion. In other words, a definable fraction of $AAIII_{IDHmut}$ fare significantly worse than a fraction of the GBM_{IDHmut}. This cannot be repaired using the current WHO nomenclature without major changes to our historical concepts of nomenclature [18].

One possible solution, which we have considered implementing in Heidelberg, would be to restrict classification to the term A_{IDHmut} and then adapt grading according to molecular lesions, thereby omitting the term GBM_{IDHmut}. The term "glioblastoma" would be reserved for

those histologically defined glioblastomas lacking IDH mutation or not having had adequate (not otherwise specified, NOS) or diagnostic (not elsewhere classified, NEC) work-ups [19]. Such a system would lend itself well to the use of layered reports, as discussed elsewhere [16]. In this context, if these data were confirmed in other studies, the WHO classification of such tumors could resemble what is given in supplementary table 2 (based on $Model_{path}$). Advantages of such an approach would include better prognostic correlations and therefore guidance of therapies, and a “freeing up” of grading from classification that could allow more easy adaptation of grading criteria in the future [18].

Conclusions

The 2016 CNS WHO grading of IDH-mutant astrocytic tumors is not as prognostically meaningful as needed and the histological parameters of proliferation and necrosis appear overrated when incorporating IDH gene status. Significantly, several other morphological and molecular parameters show higher prognostic power and modeling has provided suggestions for grading algorithms, with the proposal that *CDNK2A/B* status will be important for future grading of these tumors.

Acknowledgements

This work was supported by German Cancer Aid (70112371) to AvD and German Cancer Aid (110624) to WW and MW. We are indebted to Toshio Sasajima, Masaya Oda and Masataka Takahashi for support regarding clinical data acquisition. We thank Viktoria Zeller, Ulrike Lass, Antje Habel, Ulrike Vogel, Katja Brast, Kerstin Lindenberg, John Moyers and Jochen Meyer for excellent technical assistance. We also thank the Microarray unit of the Genomics and Proteomics Core Facility, German Cancer Research Center (DKFZ), especially Matthias Schick, Roger Fischer, Nadja Wermke and Anja Schramm-Glück, for providing methylation services.

References

1 Aoki K, Nakamura H, Suzuki H et al. (2018) Prognostic relevance of genetic alterations in diffuse lower-grade gliomas. Neuro Oncol 20: 66-77

2 Balss J, Meyer J, Mueller W, Korshunov A, Hartmann C, von Deimling A (2008) Analysis of the IDH1 codon 132 mutation in brain tumors. Acta Neuropathol 116: 597-602

3 Burger PC, Vogel FS, Green SB, Strike TA (1985) Glioblastoma multiforme and anaplastic astrocytoma, pathologic criteria and prognostic implications. Cancer 56: 1106-1111

4 Cancer Genome Atlas Research N, Brat DJ, Verhaak RG et al. (2015) Comprehensive, Integrative Genomic Analysis of Diffuse Lower-Grade Gliomas. The New England journal of medicine 372: 2481-2498

5 Capper D, Jones DTW, Sill M et al. (2018) DNA methylation-based classification of central nervous system tumours. Nature 555: 469-474

6 Capper D, Zentgraf H, Balss J, Hartmann C, von Deimling A (2009) Monoclonal Antibody Specific for IDH1 R132H Mutation. Acta Neuropathol 118: 599-601

7 Colman H, Giannini C, Huang L et al. (2006) Assessment and prognostic significance of mitotic index using the mitosis marker phospho-histone H3 in low and intermediate-grade infiltrating astrocytomas. Am J Surg Pathol 30: 657-664

8 Daumas-Duport C, Scheithauer B, O'Fallon J, Kelly P (1988) Grading of astrocytomas. A simple and reproducible method. Cancer 62: 2152-2165

9 Draaisma K, Wijnenga MM, Weenink B, Gao Y, Smid M, Robe P, van den Bent MJ, French PJ (2015) PI3 kinase mutations and mutational load as poor prognostic markers in diffuse glioma patients. Acta Neuropathol Commun 3: 88

10 Duregon E, Bertero L, Pittaro A et al. (2016) Ki-67 proliferation index but not mitotic thresholds integrates the molecular prognostic stratification of lower grade gliomas. Oncotarget 7: 21190-21198

11 Hsu DW, Louis DN, Efird JT, Hedley-Whyte ET (1997) Use of MIB-1 (Ki-67) immunoreactivity in differentiating grade II and grade III gliomas. J Neuropathol Exp Neurol 56: 857-865

12 Kernohan JW, Mabon RF, Svien HJ, Adson AW (1949) A simplified classification of gliomas. Proc Staff Meet Mayo Clin 24: 71-75

13 Louis D, Ohgaki H, Wiestler O, Cavenee W (2007) World Health Organization Classification of Tumours of the Central Nervous System. In: Bosman F, Jaffe E, Lakhani S, Ohgaki H (eds) World Health Organization Classification of Tumours 4 edn. IARC, City

14 Louis D, Ohgaki H, Wiestler O, Cavenee WK (2016) World Health Organization Classification of Tumours of the Central Nervous System. In: Bosman F, Jaffe E, Lakhani S, Ohgaki H (eds) World Health Organization Classification of Tumours Revised 4th edition edn. IARC, City

15 Louis DN, Edgerton S, Thor AD, Hedley-Whyte ET (1991) Proliferating cell nuclear antigen and Ki-67 immunohistochemistry in brain tumors: a comparative study. Acta Neuropathol 81: 675-679

16 Louis DN, Perry A, Burger P et al. (2014) International Society of Neuropathology-Haarlem Consensus Guidelines, for Nervous System Tumor Classification and Grading. Brain Pathol 24: 429-435

17 Louis DN, Perry A, Reifenberger G et al. (2016) The 2016 World Health Organization Classification of Tumors of the Central Nervous System: a summary. Acta Neuropathol 131: 803-820

18 Louis DN, von Deimling A (2017) Grading of diffuse astrocytic gliomas: Broders, Kernohan, Zulch, the WHO... and Shakespeare. Acta Neuropathol 134: 517-520

19 Louis DN, Wesseling P, Paulus W et al. (2018) cIMPACT-NOW update 1: Not Otherwise Specified (NOS) and Not Elsewhere Classified (NEC). Acta Neuropathol:

20 Olar A, Wani KM, Alfaro-Munoz KD et al. (2015) IDH mutation status and role of WHO grade and mitotic index in overall survival in grade II-III diffuse gliomas. Acta Neuropathol 129: 585-596
21 Parsons DW, Jones S, Zhang X et al. (2008) An integrated genomic analysis of human glioblastoma multiforme. Science 321: 1807-1812
22 Pekmezci M, Rice T, Molinaro AM et al. (2017) Adult infiltrating gliomas with WHO 2016 integrated diagnosis: additional prognostic roles of ATRX and TERT. Acta Neuropathol 133: 1001-1016
23 Perry A, Nobori T, Ru N, Anderl K, Borell TJ, Mohapatra G, Feuerstein BG, Jenkins RB, Carson DA (1997) Detection of p16 gene deletions in gliomas: a comparison of fluorescence in situ hybridization (FISH) versus quantitative PCR. J Neuropathol Exp Neurol 56: 999-1008
24 Pfaff E, Kessler T, Balasubramanian GP et al. (epub ahead of print) Feasibility of real-time molecular profiling for patients with newly diagnosed glioblastoma without MGMT promoter-hypermethylation - the NCT Neuro Master Match (N2M2) pilot study. Neuro Oncol:
25 Purkait S, Jha P, Sharma MC, Suri V, Sharma M, Kale SS, Sarkar C (2013) CDKN2A deletion in pediatric versus adult glioblastomas and predictive value of p16 immunohistochemistry. Neuropathology 33: 405-412
26 Reis GF, Pekmezci M, Hansen HM et al. (2015) CDKN2A loss is associated with shortened overall survival in lower-grade (World Health Organization Grades II-III) astrocytomas. J Neuropathol Exp Neurol 74: 442-452
27 Reuss DE, Kratz A, Sahm F et al. (2015) Adult IDH wild type astrocytomas biologically and clinically resolve into other tumor entities. Acta Neuropathol 130: 407-417
28 Reuss DE, Mamatjan Y, Schrimpf D et al. (2015) IDH mutant diffuse and anaplastic astrocytomas have similar age at presentation and little difference in survival: a grading problem for WHO. Acta Neuropathol 129: 867-873
29 Roy DM, Walsh LA, Desrichard A, Huse JT, Wu W, Gao J, Bose P, Lee W, Chan TA (2016) Integrated Genomics for Pinpointing Survival Loci within Arm-Level Somatic Copy Number Alterations. Cancer Cell 29: 737-750
30 Schneider CA, Rasband WS, Eliceiri KW (2012) NIH Image to ImageJ: 25 years of image analysis. Nature methods 9: 671-675
31 Sommer C, Strähle C, Köthe U, Hamprecht FA (2011) ilastik: Interactive Learning and Segmentation Toolkit. Eighth IEEE International Symposium on Biomedical Imaging (ISBI). IEEE, City, pp 230-233
32 Sturm D, Witt H, Hovestadt V et al. (2012) Hotspot Mutations in H3F3A and IDH1 Define Distinct Epigenetic and Biological Subgroups of Glioblastoma. Cancer Cell 22: 425-437
33 Suzuki H, Aoki K, Chiba K et al. (2015) Mutational landscape and clonal architecture in grade II and III gliomas. Nat Genet 47: 458-468
34 von Deimling A, Ono T, Shirahata M, Louis D (2018) Grading of Diffuse Astrocytic Gliomas: A Review of Studies Before and After the Advent of IDH Testing. Semin Neurol 38: 19-23
35 Watanabe T, Nobusawa S, Kleihues P, Ohgaki H (2009) IDH1 Mutations Are Early Events in the Development of Astrocytomas and Oligodendrogliomas. American Journal of Pathology 174: 653-656
36 Wick W, Hartmann C, Engel C et al. (2009) NOA-04 randomized phase III trial of sequential radiochemotherapy of anaplastic glioma with procarbazine, lomustine, and vincristine or temozolomide. J Clin Oncol 27: 5874-5880
37 Yan H, Parsons DW, Jin G et al. (2009) IDH1 and IDH2 Mutations in Gliomas. The New England journal of medicine 360: 765-773
38 Zülch KJ (1979) Histological typing of tumours of the central nervous system. Who‘s Who, City

Figure legends

Table 1

Morphological and clinical features and their association with OS in the discovery set.

Table 2

Genes with amplifications or homozygous deletions found in 211 IDH-mutated astrocytomas in the discovery set and their association with OS. Univarate analysis.

Figure 1

Kaplan-Meier plot stratifying according to WHO in the discovery set (a). (b) shows the same patients with additional stratification for homozygous deletion of *CDKN2A/B*.

Figure 2

Distribution of 211 patients in the discovery set according to WHO grading and to three different grading approaches. N+ ~ necrosis present; N- ~ necrosis absent; P+ ~ CDKN2A/B is homozygously deleted; P- ~ CDKN2A/B is not homozygously deleted; C+ ~ high CNVL-load; C- ~ low CNVL-load. Parameter P+ is not encountered in AII_{IDHmut} and, therefore, this potential tumor subset is not depicted in the three alternative grading approaches.
Top: Grading model applied. Middle: Placement of patient groups with distinct features according to the four different approaches. Bottom: OS of patients according to the four approaches.

Figure 3

Kaplan-Meier plots stratifying according to WHO, $Model_{path}$ and $Model_{CNVL}$ and $Model_{combined}$ in the discovery set (a, b, c, d), the HD validation set (e, f, g, h) the EORTC validation set (i, j, k, l) and the TCGA set (m, n, o, p).
Coulor schemes for WHO: red GBM_{IDHmut}, blue $AAIII_{IDHmut}$, green AII_{IDHmut}; for $Model_{path}$: red A4, blue $A3_{path}$, green $A2_{path}$; for $Model_{CNVL}$: red A4, blue $A3_{CNVL}$, green $A2_{CNVL}$; for $Model_{combined}$: red A4, blue $A3_{combined}$, green $A2_{comined.}$

Figure 4

Brier scores to the grading approaches in the discovery set (a) and HD-validation set (b): reference which was random distribution (black), classifier tool (orange) based on epigenomic classification[5], unsupervised clustering of 850K based methylation data (yellow), WHO diagnosis (red), $Model_{path}$ (blue), $Model_{CNVL}$ (green) and $Model_{combined}$ (purple.)

Supplementary table 1

Discovery set data employed in grading schemes for IDH-mutant astrocytoma. For each scheme lowest grade is indicated by green, intermediate grade by blue and highest grade by red color.

Supplementary Table 2

Possible designation of IDH-mutant astrocytoma based on $Model_{path}$ in a future classification scheme

Supplementary figure 1

Copy number summary plots. Vertical axis indicates percentage of patients affected. Horizontal axis refers to chromosomal localization. Dotted vertical lines indicate border between p and q arms. Data are given for three age groups.

Supplementary figure 2

Kaplan-Meier plots stratifying by unsupervised clustering in the discovery set (a), the HD validation set (b) and the EORTC validation set (c).
Kaplan-Meier plots stratifying by the methylation based classifier in the discovery set (d), the HD validation set (e) and the EORTC validation set (f).

Supplementary figure 3

OS of subgroups in $Model_{combined}$. The patient set (n = 7) characterized by necrosis, absence of CDKN2A/B homozygous deletion and low CNVL exhibited only 2 events. While the corresponding curve (red) fits well the group of patients with intermediate OS, the number is too low for a clear statement.

Supplementary figure 4

Association of proliferation markers with CDKN2A/B status. (a) association with Ki67. (b) association with pHH3. Horizontal bars in box-plots correspond to median values.

Supplementary figure 5

OS of patients with IDH-mutant astrocytoma in association with RB pathway genes. (a) red - homozygous deletion of CDKN2A/B, black – wild type status. (b) red –homozygous deletion of RB1 or CDK4 amplification or CDK6 amplification, black – wild type status. . (a) red - homozygous deletion of CDKN2A/B or homozygous deletion of RB1 or CDK4 amplification or CDK6 amplification, black – wild type status for all.

Supplementary figure 6

Examples for CNP from astrocytic tumors exhibiting homozygous deletion of CDKN2A/B.

Figure 1

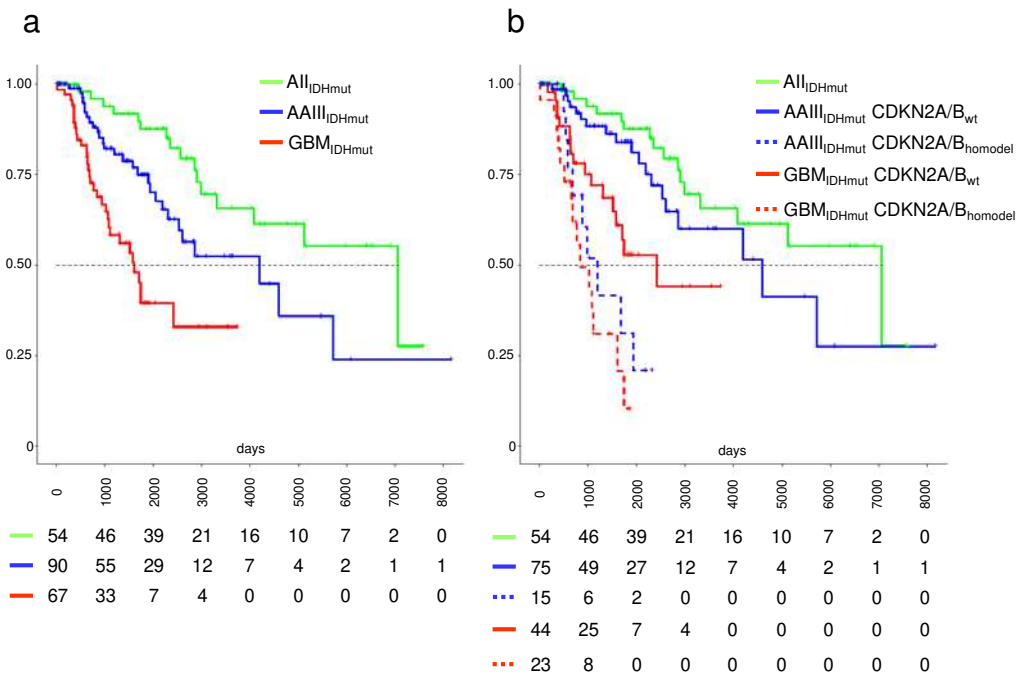
a
b
1.00
0.75
0.50
0.25
0
days
0
1000
2000
3000
4000
5000
6000
7000
8000
AII IDHmut
AAIII IDHmut
GBM IDHmut
AAIII IDHmut CDKN2A/B wt
AAIII IDHmut CDKN2A/B homodel
GBM IDHmut CDKN2A/B wt
GBM IDHmut CDKN2A/B homodel
54 46 39 21 16 10 7 2 0
90 55 29 12 7 4 2 1 1
67 33 7 4 0 0 0 0 0
54 46 39 21 16 10 7 2 0
75 49 27 12 7 4 2 1 1
15 6 2 0 0 0 0 0 0
44 25 7 4 0 0 0 0 0
23 8 0 0 0 0 0 0 0

Figure 2

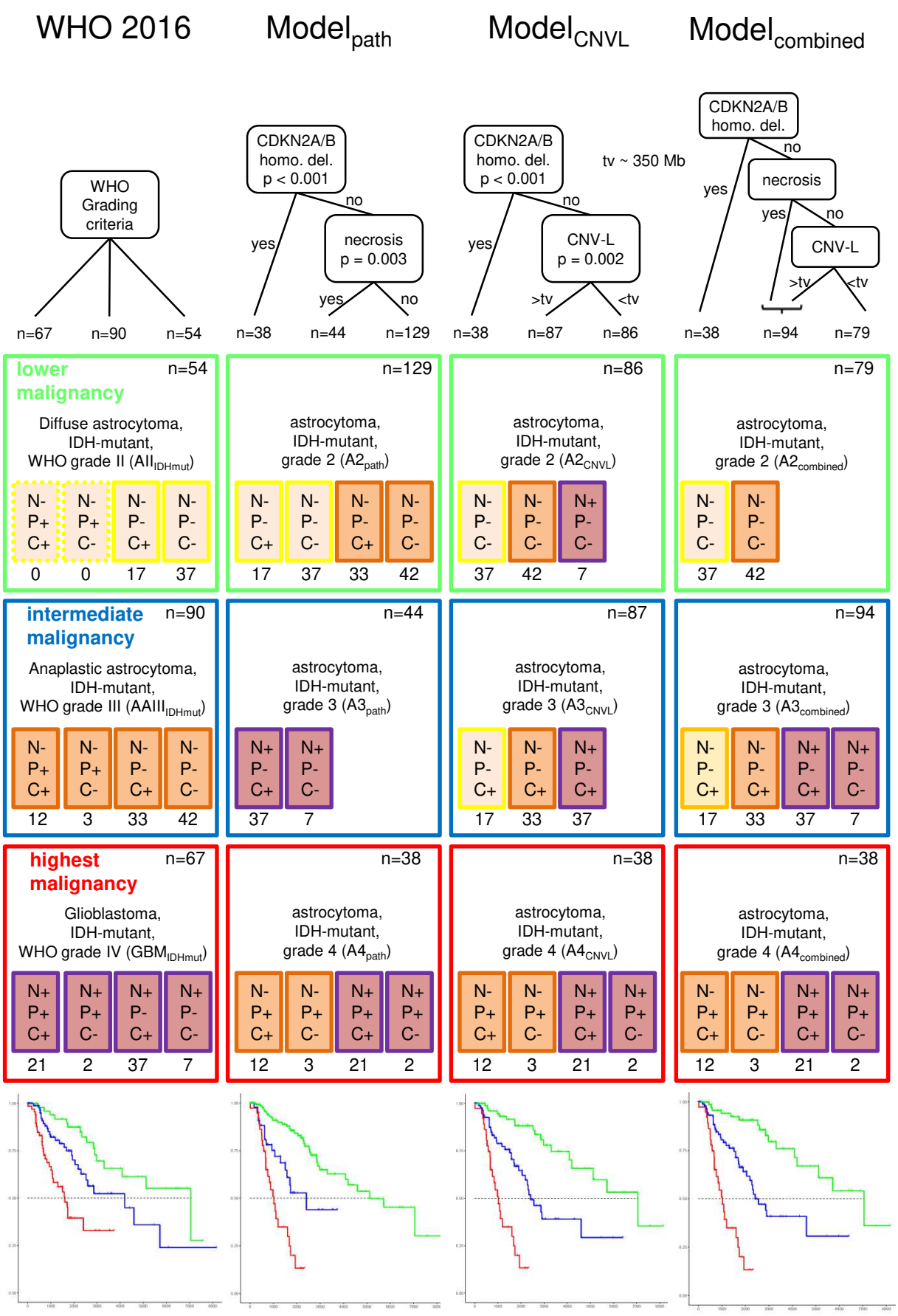
WHO 2016
Model$_{path}$
Model$_{CNVL}$
Model$_{combined}$
WHO Grading criteria
n=67
n=90
n=54
CDKN2A/B homo. del. p < 0.001
yes
no
necrosis p = 0.003
yes
no
n=38
n=44
n=129
CDKN2A/B homo. del. p < 0.001
yes
no
CNV-L p = 0.002
>tv
<tv
n=38
n=87
n=86
tv ~ 350 Mb
CDKN2A/B homo. del.
yes
no
necrosis
yes
no
CNV-L
>tv
<tv
n=38
n=94
n=79
lower malignancy
n=54
Diffuse astrocytoma, IDH-mutant, WHO grade II (AII$_{IDHmut}$)
N- P+ C+ 0
N- P+ C- 0
N- P- C+ 17
N- P- C- 37
n=129
astrocytoma, IDH-mutant, grade 2 (A2$_{path}$)
N- P- C+ 17
N- P- C- 37
N- P- C+ 33
N- P- C- 42
n=86
astrocytoma, IDH-mutant, grade 2 (A2$_{CNVL}$)
N- P- C- 37
N- P- C- 42
N+ P- C- 7
n=79
astrocytoma, IDH-mutant, grade 2 (A2$_{combined}$)
N- P- C- 37
N- P- C- 42
intermediate malignancy
n=90
Anaplastic astrocytoma, IDH-mutant, WHO grade III (AAIII$_{IDHmut}$)
N- P+ C+ 12
N- P+ C- 3
N- P- C+ 33
N- P- C- 42
n=44
astrocytoma, IDH-mutant, grade 3 (A3$_{path}$)
N+ P- C+ 37
N+ P- C- 7
n=87
astrocytoma, IDH-mutant, grade 3 (A3$_{CNVL}$)
N- P- C+ 17
N- P- C+ 33
N+ P- C+ 37
n=94
astrocytoma, IDH-mutant, grade 3 (A3$_{combined}$)
N- P- C+ 17
N- P- C+ 33
N+ P- C+ 37
N+ P- C- 7
highest malignancy
n=67
Glioblastoma, IDH-mutant, WHO grade IV (GBM$_{IDHmut}$)
N+ P+ C+ 21
N+ P+ C- 2
N+ P- C+ 37
N+ P- C- 7
n=38
astrocytoma, IDH-mutant, grade 4 (A4$_{path}$)
N- P+ C+ 12
N- P+ C- 3
N+ P+ C+ 21
N+ P+ C- 2
n=38
astrocytoma, IDH-mutant, grade 4 (A4$_{CNVL}$)
N- P+ C+ 12
N- P+ C- 3
N+ P+ C+ 21
N+ P+ C- 2
n=38
astrocytoma, IDH-mutant, grade 4 (A4$_{combined}$)
N- P+ C+ 12
N- P+ C- 3
N+ P+ C+ 21
N+ P+ C- 2

Figure 3

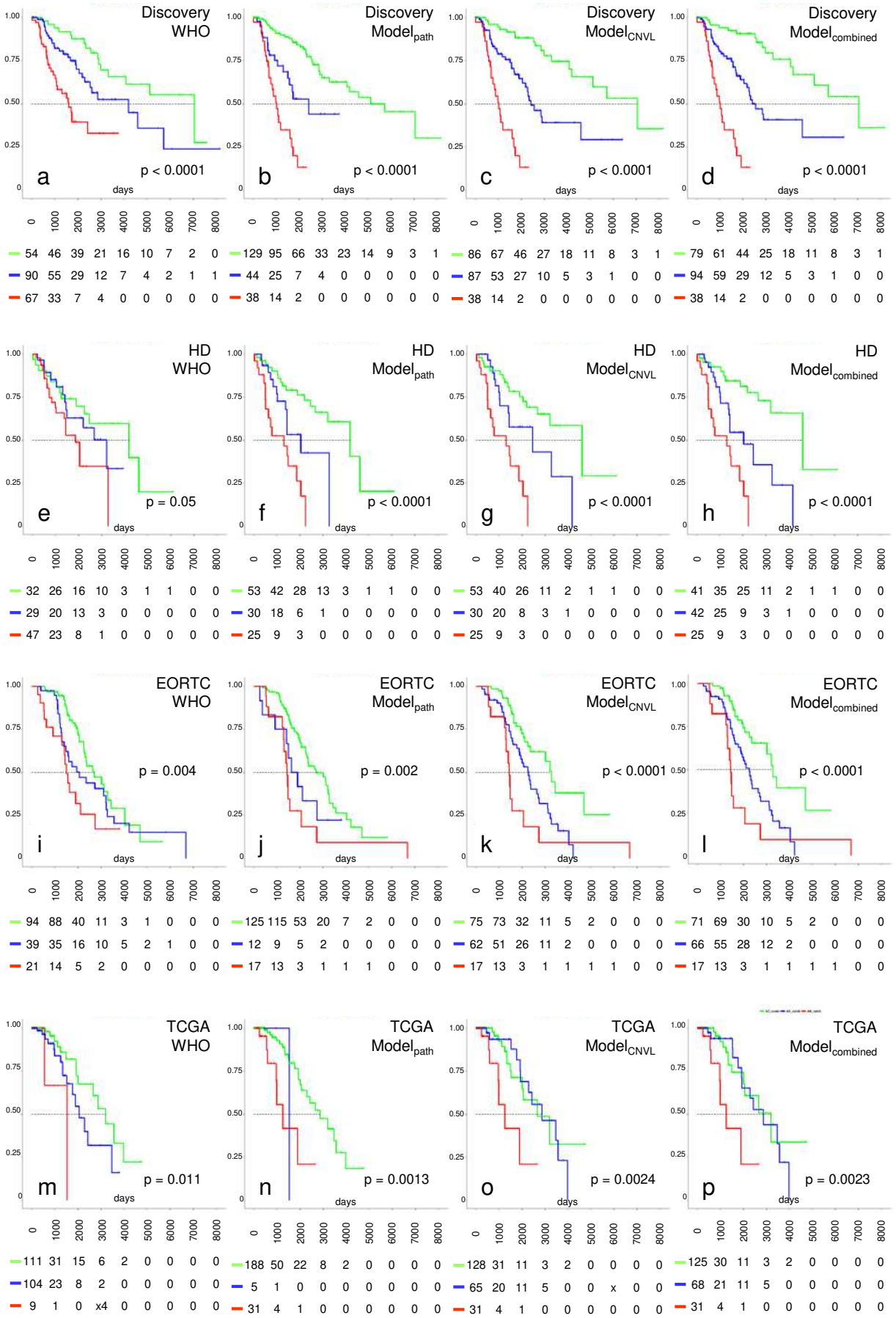
Discovery WHO
a
p < 0.0001
days
54 46 39 21 16 10 7 2 0
90 55 29 12 7 4 2 1 1
67 33 7 4 0 0 0 0 0
Discovery Model$_{path}$
b
p < 0.0001
days
129 95 66 33 23 14 9 3 1
44 25 7 4 0 0 0 0 0
38 14 2 0 0 0 0 0 0
Discovery Model$_{CNVL}$
c
p < 0.0001
days
86 67 46 27 18 11 8 3 1
87 53 27 10 5 3 1 0 0
38 14 2 0 0 0 0 0 0
Discovery Model$_{combined}$
d
p < 0.0001
days
79 61 44 25 18 11 8 3 1
94 59 29 12 5 3 1 0 0
38 14 2 0 0 0 0 0 0
HD WHO
e
p = 0.05
days
32 26 16 10 3 1 1 0 0
29 20 13 3 0 0 0 0 0
47 23 8 1 0 0 0 0 0
HD Model$_{path}$
f
p < 0.0001
days
53 42 28 13 3 1 1 0 0
30 18 6 1 0 0 0 0 0
25 9 3 0 0 0 0 0 0
HD Model$_{CNVL}$
g
p < 0.0001
days
53 40 26 11 2 1 1 0 0
30 20 8 3 1 0 0 0 0
25 9 3 0 0 0 0 0 0
HD Model$_{combined}$
h
p < 0.0001
days
41 35 25 11 2 1 1 0 0
42 25 9 3 1 0 0 0 0
25 9 3 0 0 0 0 0 0
EORTC WHO
i
p = 0.004
days
94 88 40 11 3 1 0 0 0
39 35 16 10 5 2 1 0 0
21 14 5 2 0 0 0 0 0
EORTC Model$_{path}$
j
p = 0.002
days
125 115 53 20 7 2 0 0 0
12 9 5 2 0 0 0 0 0
17 13 3 1 1 1 0 0 0
EORTC Model$_{CNVL}$
k
p < 0.0001
days
75 73 32 11 5 2 0 0 0
62 51 26 11 2 0 0 0 0
17 13 3 1 1 1 1 0 0
EORTC Model$_{combined}$
l
p < 0.0001
days
71 69 30 10 5 2 0 0 0
66 55 28 12 2 0 0 0 0
17 13 3 1 1 1 1 0 0
TCGA WHO
m
p = 0.011
days
111 31 15 6 2 0 0 0 0
104 23 8 2 0 0 0 0 0
9 1 0 x4 0 0 0 0 0
TCGA Model$_{path}$
n
p = 0.0013
days
188 50 22 8 2 0 0 0 0
5 1 0 0 0 0 0 0 0
31 4 1 0 0 0 0 0 0
TCGA Model$_{CNVL}$
o
p = 0.0024
days
128 31 11 3 2 0 0 0 0
65 20 11 5 0 0 x 0 0
31 4 1 0 0 0 0 0 0
TCGA Model$_{combined}$
p
p = 0.0023
days
125 30 11 3 2 0 0 0 0
68 21 11 5 0 0 0 0 0
31 4 1 0 0 0 0 0 0

Figure 4

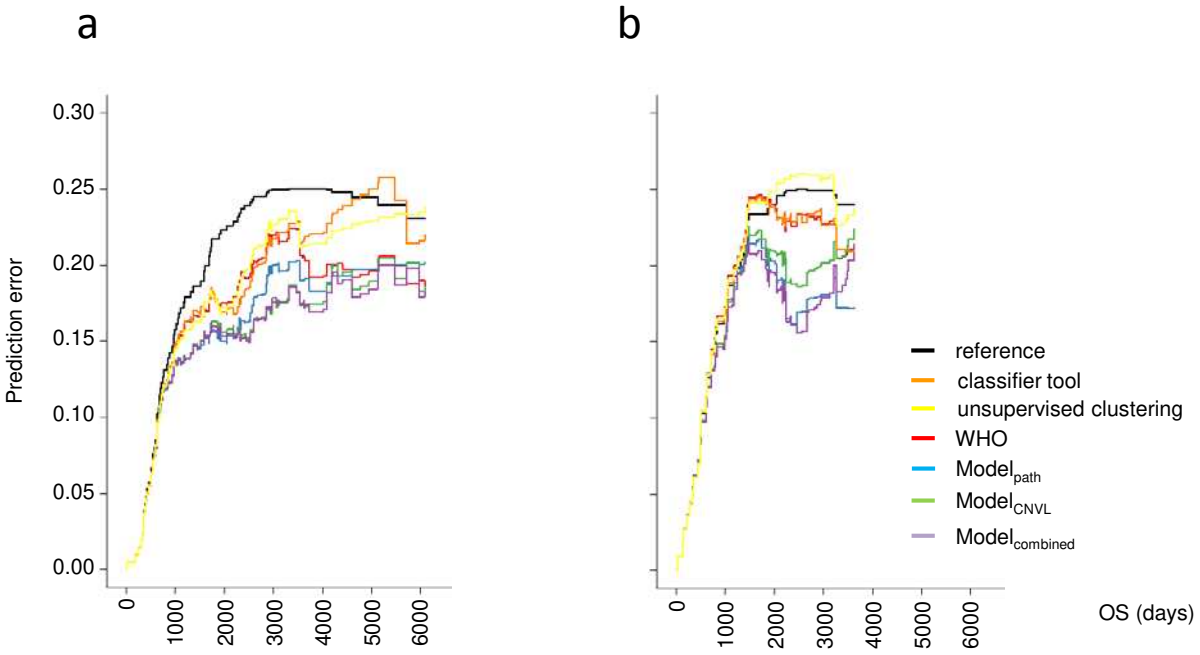
a
b
Prediction error
0.30
0.25
0.20
0.15
0.10
0.05
0.00
0
1000
2000
3000
4000
5000
6000
reference
classifier tool
unsupervised clustering
WHO
Model$_{path}$
Model$_{CNVL}$
Model$_{combined}$
OS (days)

Supplementary figure 1

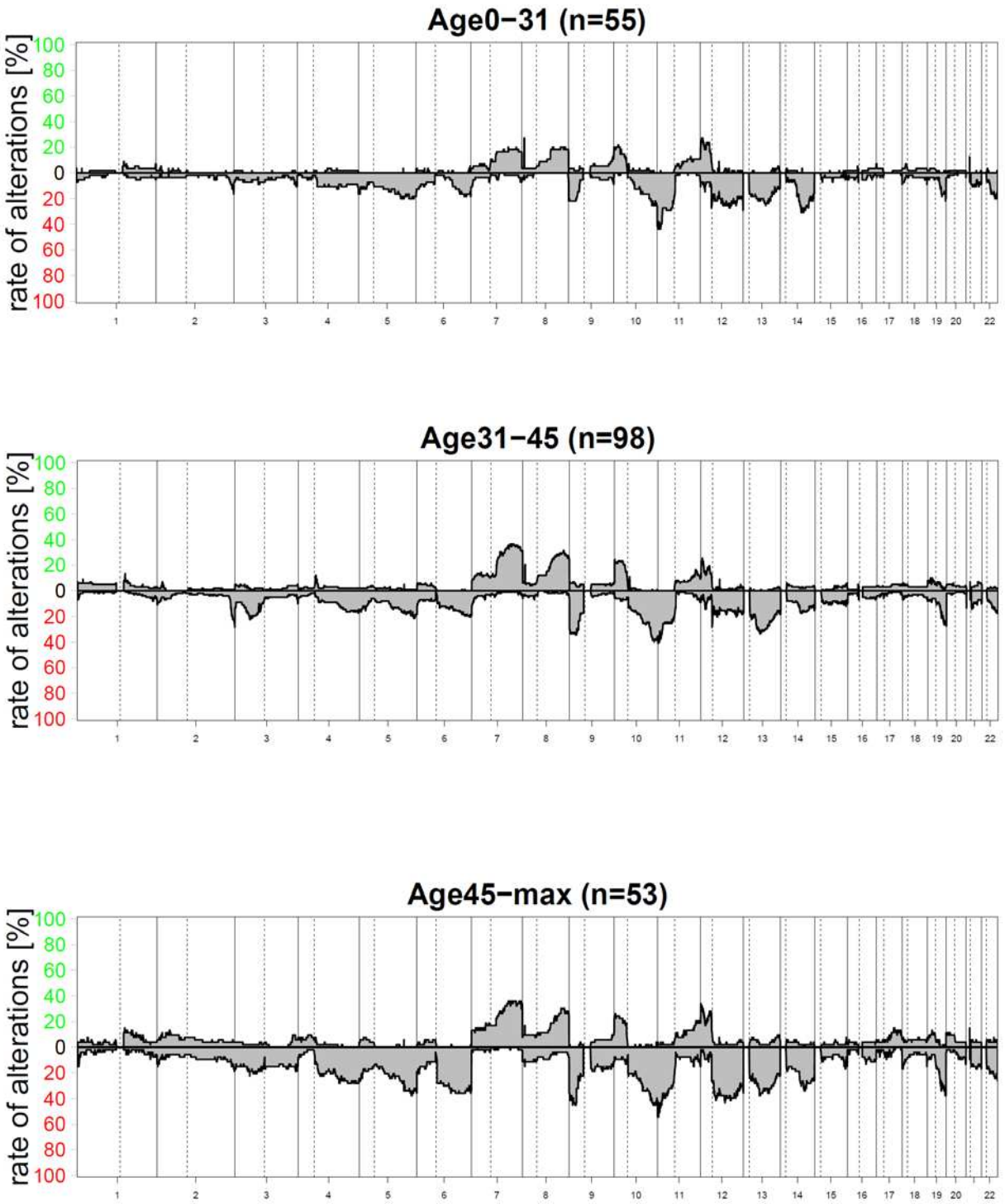

Supplementary figure 2

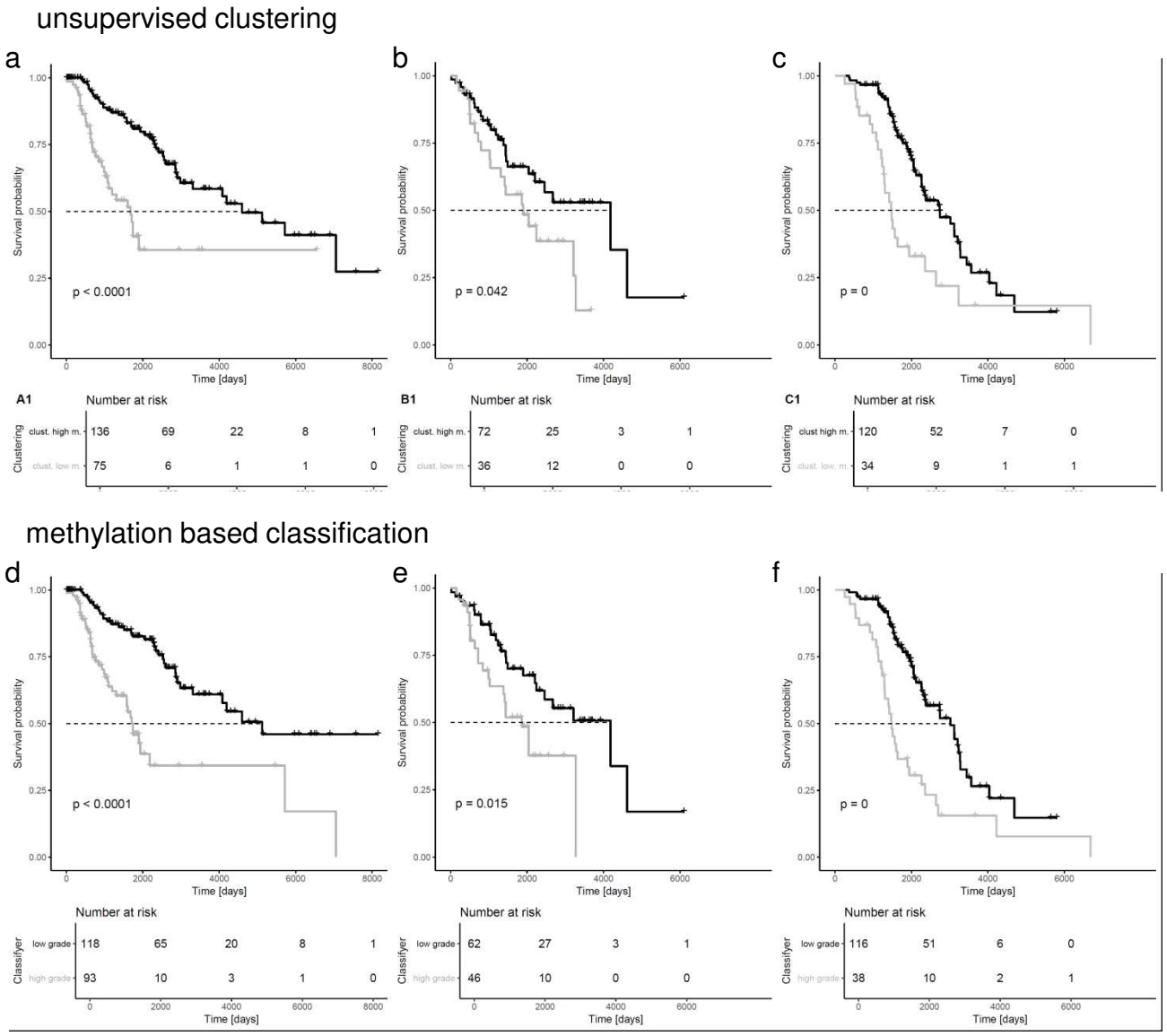

Supplementary figure 3

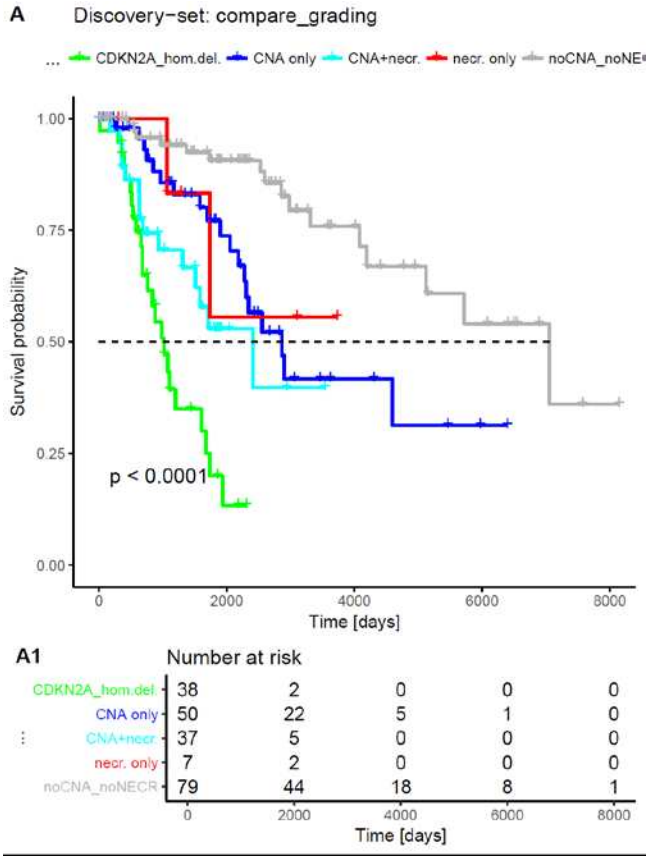

Supplementary figure 4

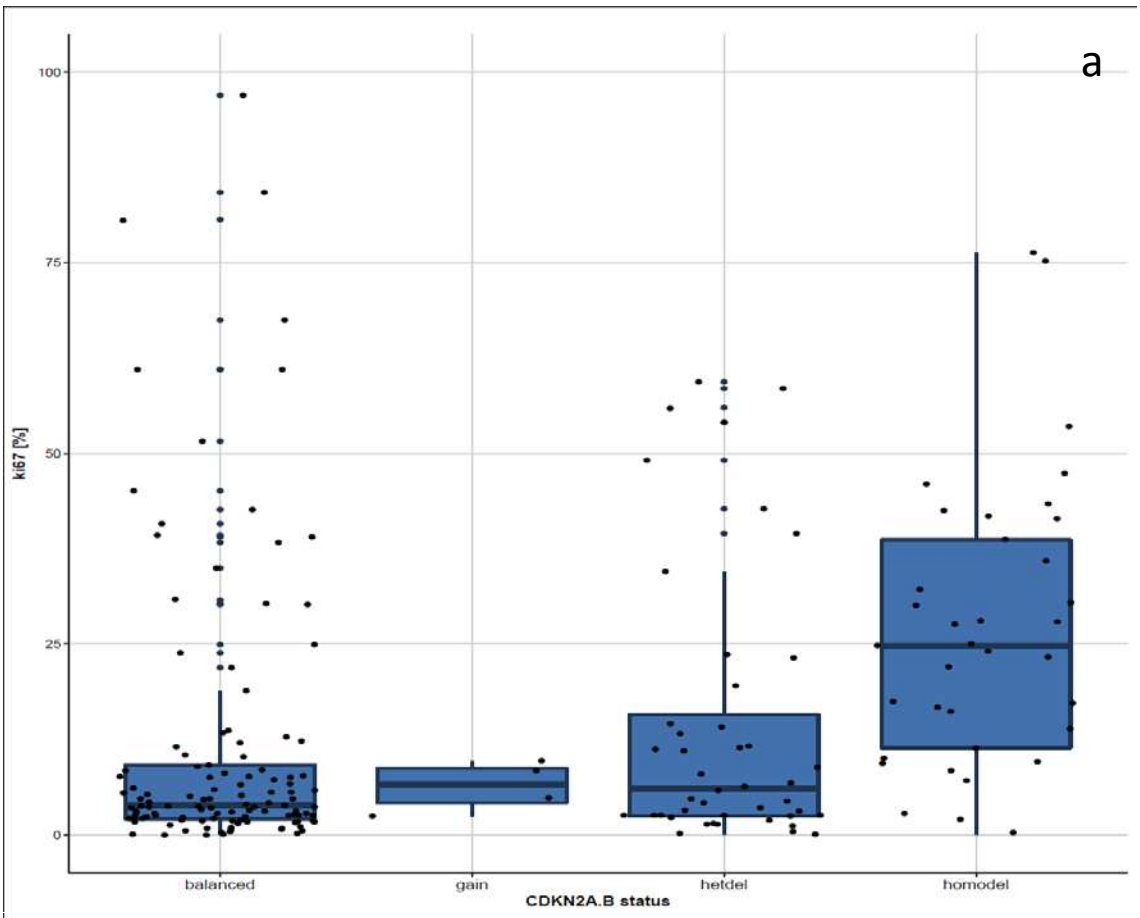

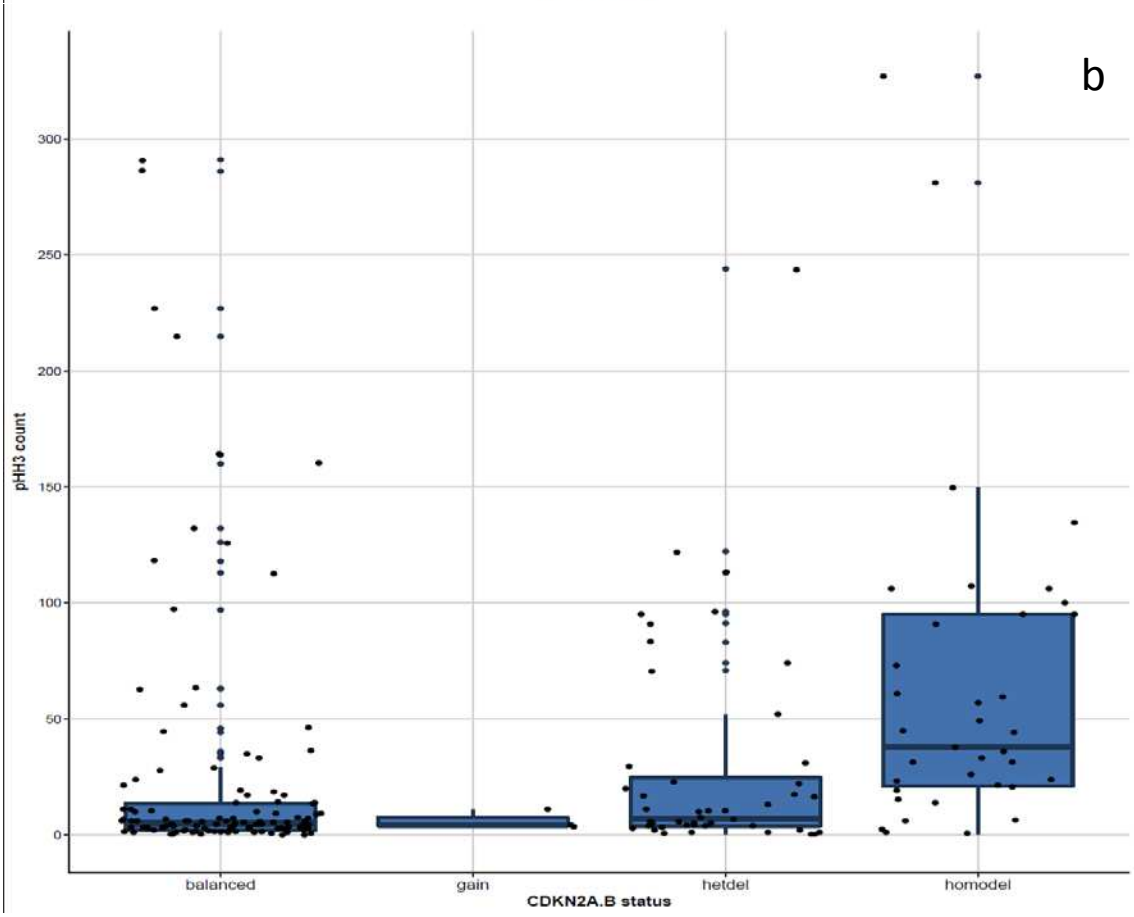

Supplementary figure 5

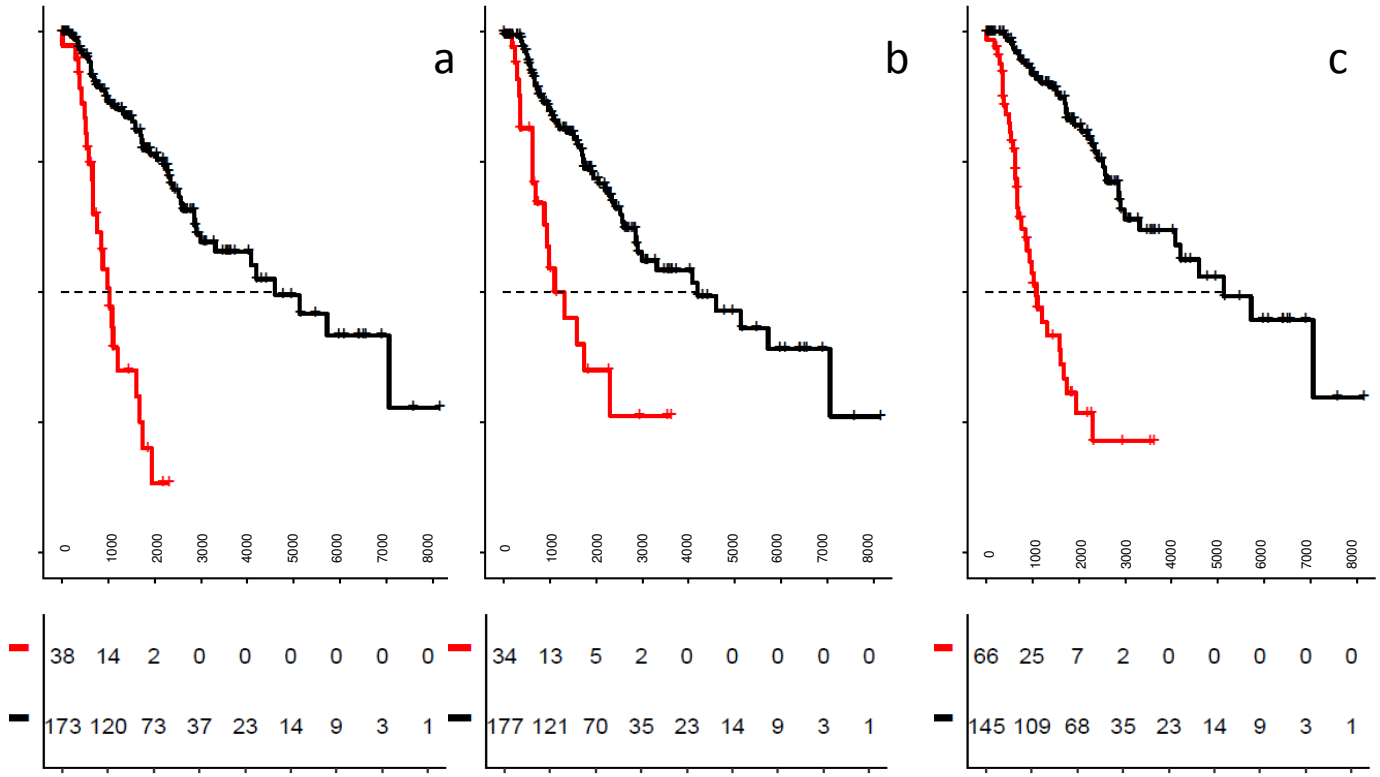

Supplementary figure 6

Case 71520

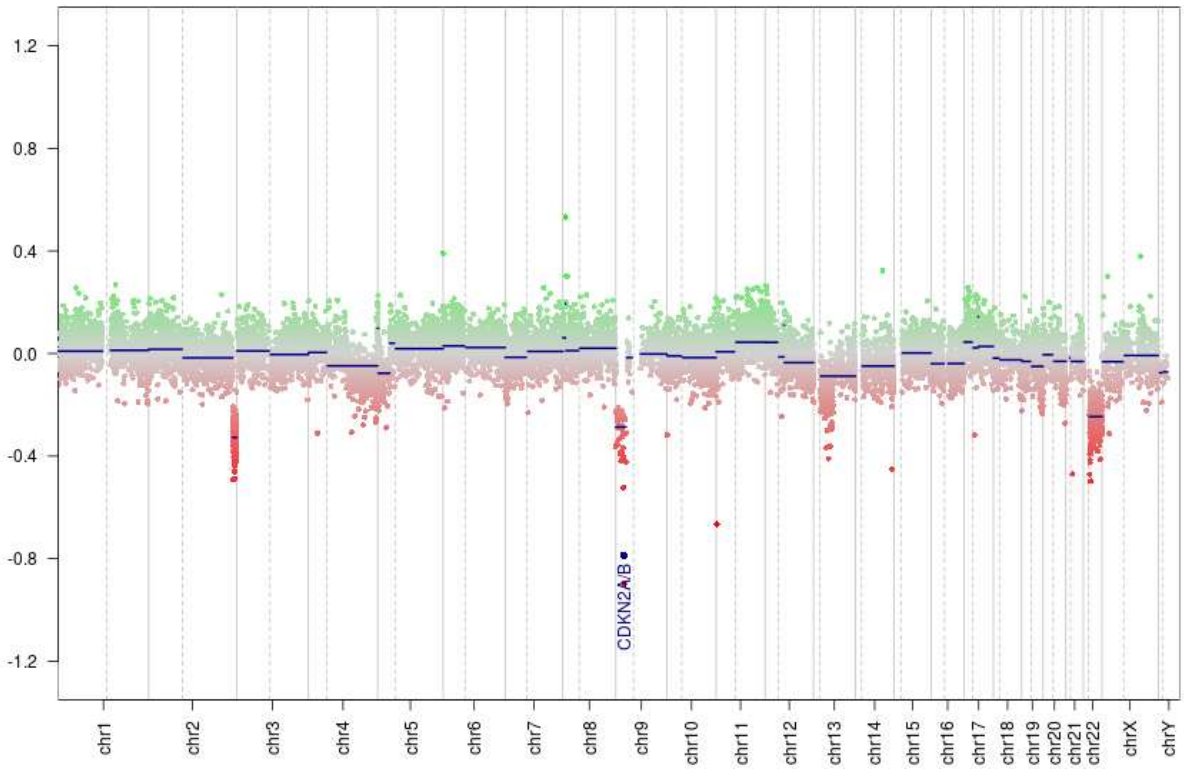

Case 67256

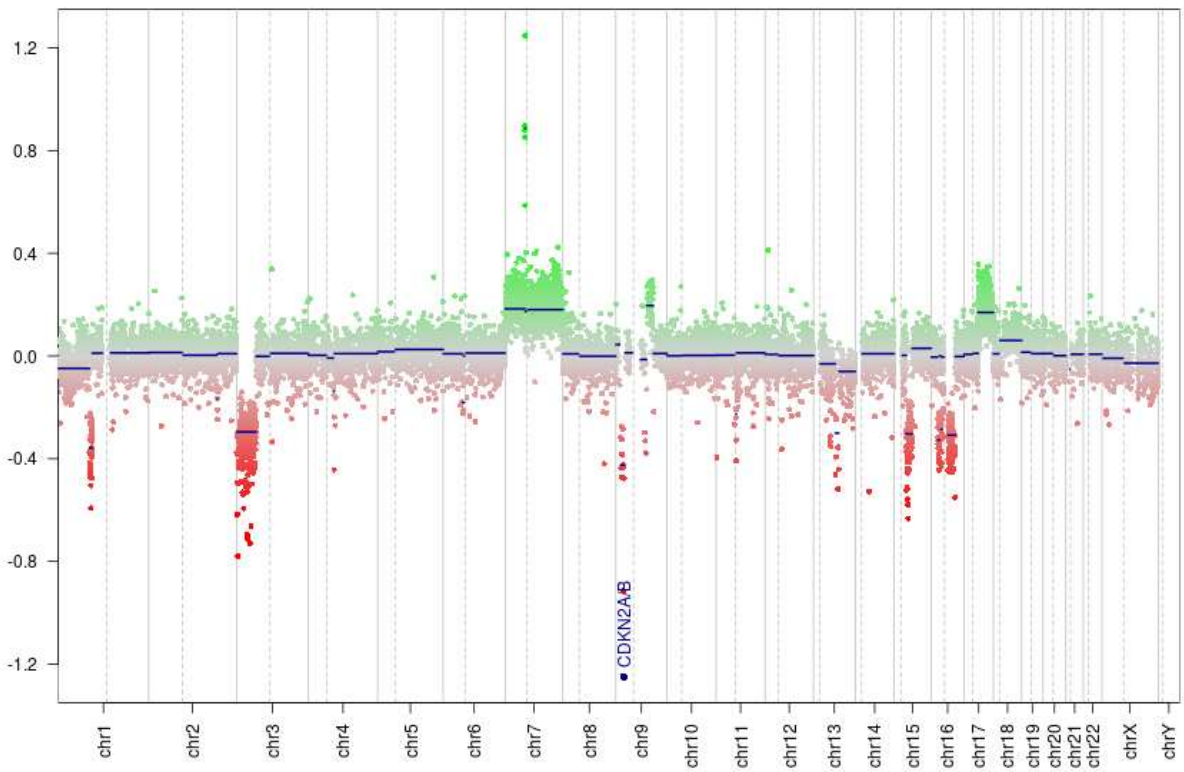

Supplementary Table 1

case	Age	gender	WHO	OS	CDKN2A/B	Necrosis	CNVL (bp)	$Model_{path}$	$Model_{CNVL}$	$Model_{combined}$
1	37	f	All_{IDHmut}	4022	balanced	no	276499911	$A2_{path}$	$A2_{CNVL}$	$A2_{combined}$
2	51	f	All_{IDHmut}	3275	balanced	no	275244442	$A2_{path}$	$A2_{CNVL}$	$A2_{combined}$
3	26	m	All_{IDHmut}	7053	hetdel	no	118472068	$A2_{path}$	$A2_{CNVL}$	$A2_{combined}$
4	28	f	All_{IDHmut}	6497	balanced	no	100902350	$A2_{path}$	$A2_{CNVL}$	$A2_{combined}$
5	24	m	All_{IDHmut}	5122	hetdel	no	12386106	$A2_{path}$	$A2_{CNVL}$	$A2_{combined}$
6	23	f	All_{IDHmut}	1731	balanced	no	274819415	$A2_{path}$	$A2_{CNVL}$	$A2_{combined}$
7	54	f	All_{IDHmut}	2700	hetdel	no	32231326	$A2_{path}$	$A2_{CNVL}$	$A2_{combined}$
8	29	m	All_{IDHmut}	448	balanced	no	54866147	$A2_{path}$	$A2_{CNVL}$	$A2_{combined}$
9	38	f	All_{IDHmut}	2314	balanced	no	228565769	$A2_{path}$	$A2_{CNVL}$	$A2_{combined}$
10	46	m	All_{IDHmut}	1481	balanced	no	304920289	$A2_{path}$	$A2_{CNVL}$	$A2_{combined}$
11	25	m	All_{IDHmut}	4207	balanced	no	120631604	$A2_{path}$	$A2_{CNVL}$	$A2_{combined}$
12	29	f	All_{IDHmut}	2190	balanced	no	305279829	$A2_{path}$	$A2_{CNVL}$	$A2_{combined}$
13	38	f	All_{IDHmut}	1917	balanced	no	147031947	$A2_{path}$	$A2_{CNVL}$	$A2_{combined}$
14	43	m	All_{IDHmut}	2852	hetdel	no	214674094	$A2_{path}$	$A2_{CNVL}$	$A2_{combined}$
15	26	f	All_{IDHmut}	129	balanced	no	73687679	$A2_{path}$	$A2_{CNVL}$	$A2_{combined}$
16	31	f	All_{IDHmut}	3310	balanced	no	166849942	$A2_{path}$	$A2_{CNVL}$	$A2_{combined}$
17	31	f	All_{IDHmut}	4769	balanced	no	157179197	$A2_{path}$	$A2_{CNVL}$	$A2_{combined}$
18	50	f	All_{IDHmut}	6896	balanced	no	306090692	$A2_{path}$	$A2_{CNVL}$	$A2_{combined}$
19	25	f	All_{IDHmut}	2769	balanced	no	87857691	$A2_{path}$	$A2_{CNVL}$	$A2_{combined}$
20	36	m	All_{IDHmut}	3110	balanced	no	134873237	$A2_{path}$	$A2_{CNVL}$	$A2_{combined}$
21	43	m	All_{IDHmut}	5151	balanced	no	296069657	$A2_{path}$	$A2_{CNVL}$	$A2_{combined}$
22	32	m	All_{IDHmut}	4947	balanced	no	318517227	$A2_{path}$	$A2_{CNVL}$	$A2_{combined}$
23	46	m	All_{IDHmut}	4083	hetdel	no	211988482	$A2_{path}$	$A2_{CNVL}$	$A2_{combined}$
24	28	f	All_{IDHmut}	2877	balanced	no	63527897	$A2_{path}$	$A2_{CNVL}$	$A2_{combined}$
25	25	m	All_{IDHmut}	968	balanced	no	90983369	$A2_{path}$	$A2_{CNVL}$	$A2_{combined}$
26	28	m	All_{IDHmut}	2980	hetdel	no	272577994	$A2_{path}$	$A2_{CNVL}$	$A2_{combined}$
27	28	f	All_{IDHmut}	3624	balanced	no	97759160	$A2_{path}$	$A2_{CNVL}$	$A2_{combined}$
28	26	m	All_{IDHmut}	6411	balanced	no	42297630	$A2_{path}$	$A2_{CNVL}$	$A2_{combined}$
29	34	f	All_{IDHmut}	7574	balanced	no	80568258	$A2_{path}$	$A2_{CNVL}$	$A2_{combined}$
30	35	f	All_{IDHmut}	2270	balanced	no	201135535	$A2_{path}$	$A2_{CNVL}$	$A2_{combined}$
31	26	m	All_{IDHmut}	6549	balanced	no	1875847	$A2_{path}$	$A2_{CNVL}$	$A2_{combined}$
32	52	f	All_{IDHmut}	1849	balanced	no	208322963	$A2_{path}$	$A2_{CNVL}$	$A2_{combined}$
33	36	m	All_{IDHmut}	2074	hetdel	no	298249331	$A2_{path}$	$A2_{CNVL}$	$A2_{combined}$
34	39	f	All_{IDHmut}	21	balanced	no	40784782	$A2_{path}$	$A2_{CNVL}$	$A2_{combined}$
35	31	m	All_{IDHmut}	100	hetdel	no	234203374	$A2_{path}$	$A2_{CNVL}$	$A2_{combined}$
36	31	m	All_{IDHmut}	2182	hetdel	no	246267203	$A2_{path}$	$A2_{CNVL}$	$A2_{combined}$
37	29	m	All_{IDHmut}	2297	balanced	no	97150870	$A2_{path}$	$A2_{CNVL}$	$A2_{combined}$
38	38	f	All_{IDHmut}	2342	balanced	no	633608335	$A2_{path}$	$A3_{CNVL}$	$A3_{combined}$
39	32	m	All_{IDHmut}	2556	balanced	no	442770300	$A2_{path}$	$A3_{CNVL}$	$A3_{combined}$
40	28	f	All_{IDHmut}	6394	gain	no	440940501	$A2_{path}$	$A3_{CNVL}$	$A3_{combined}$
41	30	f	All_{IDHmut}	4302	hetdel	no	763615945	$A2_{path}$	$A3_{CNVL}$	$A3_{combined}$
42	37	m	All_{IDHmut}	1693	balanced	no	358458133	$A2_{path}$	$A3_{CNVL}$	$A3_{combined}$
43	46	f	All_{IDHmut}	1104	balanced	no	426876972	$A2_{path}$	$A3_{CNVL}$	$A3_{combined}$
44	29	m	All_{IDHmut}	2491	balanced	no	430413652	$A2_{path}$	$A3_{CNVL}$	$A3_{combined}$

45	51	m	AII_{IDHmut}	2901	hetdel	no	526514536	$A2_{path}$	$A3_{CNVL}$	$A3_{combined}$
46	70	f	AII_{IDHmut}	709	balanced	no	377719470	$A2_{path}$	$A3_{CNVL}$	$A3_{combined}$
47	46	m	AII_{IDHmut}	3058	balanced	no	403543802	$A2_{path}$	$A3_{CNVL}$	$A3_{combined}$
48	67	f	AII_{IDHmut}	2672	hetdel	no	836373426	$A2_{path}$	$A3_{CNVL}$	$A3_{combined}$
49	51	f	AII_{IDHmut}	2219	hetdel	no	646859920	$A2_{path}$	$A3_{CNVL}$	$A3_{combined}$
50	29	m	AII_{IDHmut}	2278	balanced	no	484645537	$A2_{path}$	$A3_{CNVL}$	$A3_{combined}$
51	41	m	AII_{IDHmut}	5971	hetdel	no	704332454	$A2_{path}$	$A3_{CNVL}$	$A3_{combined}$
52	41	m	AII_{IDHmut}	228	balanced	no	662264513	$A2_{path}$	$A3_{CNVL}$	$A3_{combined}$
53	67	f	AII_{IDHmut}	1173	balanced	no	572896836	$A2_{path}$	$A3_{CNVL}$	$A3_{combined}$
54	34	m	AII_{IDHmut}	379	balanced	no	406233411	$A2_{path}$	$A3_{CNVL}$	$A3_{combined}$
55	35	f	$AAIII_{IDHmut}$	363	hetdel	no	178096653	$A2_{path}$	$A2_{CNVL}$	$A2_{combined}$
56	22	m	$AAIII_{IDHmut}$	3641	hetdel	no	197533690	$A2_{path}$	$A2_{CNVL}$	$A2_{combined}$
57	26	m	$AAIII_{IDHmut}$	6081	hetdel	no	103568330	$A2_{path}$	$A2_{CNVL}$	$A2_{combined}$
58	35	m	$AAIII_{IDHmut}$	2598	balanced	no	200733683	$A2_{path}$	$A2_{CNVL}$	$A2_{combined}$
59	42	f	$AAIII_{IDHmut}$	2661	balanced	no	132505213	$A2_{path}$	$A2_{CNVL}$	$A2_{combined}$
60	32	m	$AAIII_{IDHmut}$	664	balanced	no	104349865	$A2_{path}$	$A2_{CNVL}$	$A2_{combined}$
61	32	f	$AAIII_{IDHmut}$	422	hetdel	no	187991641	$A2_{path}$	$A2_{CNVL}$	$A2_{combined}$
62	37	f	$AAIII_{IDHmut}$	1758	gain	no	304204478	$A2_{path}$	$A2_{CNVL}$	$A2_{combined}$
63	42	f	$AAIII_{IDHmut}$	1219	gain	no	187801981	$A2_{path}$	$A2_{CNVL}$	$A2_{combined}$
64	26	m	$AAIII_{IDHmut}$	1691	balanced	no	145503063	$A2_{path}$	$A2_{CNVL}$	$A2_{combined}$
65	25	m	$AAIII_{IDHmut}$	1488	balanced	no	207787601	$A2_{path}$	$A2_{CNVL}$	$A2_{combined}$
66	31	f	$AAIII_{IDHmut}$	1033	hetdel	no	315520776	$A2_{path}$	$A2_{CNVL}$	$A2_{combined}$
67	35	m	$AAIII_{IDHmut}$	1444	balanced	no	255473408	$A2_{path}$	$A2_{CNVL}$	$A2_{combined}$
68	25	f	$AAIII_{IDHmut}$	41	balanced	no	283494206	$A2_{path}$	$A2_{CNVL}$	$A2_{combined}$
69	36	m	$AAIII_{IDHmut}$	146	balanced	no	42705800	$A2_{path}$	$A2_{CNVL}$	$A2_{combined}$
70	55	m	$AAIII_{IDHmut}$	546	balanced	no	6385695	$A2_{path}$	$A2_{CNVL}$	$A2_{combined}$
71	35	f	$AAIII_{IDHmut}$	961	balanced	no	245265283	$A2_{path}$	$A2_{CNVL}$	$A2_{combined}$
72	35	m	$AAIII_{IDHmut}$	1371	balanced	no	194100168	$A2_{path}$	$A2_{CNVL}$	$A2_{combined}$
73	42	f	$AAIII_{IDHmut}$	1892	balanced	no	169361691	$A2_{path}$	$A2_{CNVL}$	$A2_{combined}$
74	37	f	$AAIII_{IDHmut}$	1772	balanced	no	107496655	$A2_{path}$	$A2_{CNVL}$	$A2_{combined}$
75	37	m	$AAIII_{IDHmut}$	1289	balanced	no	173539970	$A2_{path}$	$A2_{CNVL}$	$A2_{combined}$
76	31	m	$AAIII_{IDHmut}$	3089	balanced	no	88952640	$A2_{path}$	$A2_{CNVL}$	$A2_{combined}$
77	36	f	$AAIII_{IDHmut}$	2911	balanced	no	143626885	$A2_{path}$	$A2_{CNVL}$	$A2_{combined}$
78	37	m	$AAIII_{IDHmut}$	2843	balanced	no	178612373	$A2_{path}$	$A2_{CNVL}$	$A2_{combined}$
79	30	m	$AAIII_{IDHmut}$	4194	balanced	no	337431093	$A2_{path}$	$A2_{CNVL}$	$A2_{combined}$
80	36	m	$AAIII_{IDHmut}$	3583	balanced	no	77900000	$A2_{path}$	$A2_{CNVL}$	$A2_{combined}$
81	61	m	$AAIII_{IDHmut}$	586	balanced	no	209203001	$A2_{path}$	$A2_{CNVL}$	$A2_{combined}$
82	20	f	$AAIII_{IDHmut}$	2621	balanced	no	76220792	$A2_{path}$	$A2_{CNVL}$	$A2_{combined}$
83	32	m	$AAIII_{IDHmut}$	5716	balanced	no	196477555	$A2_{path}$	$A2_{CNVL}$	$A2_{combined}$
84	36	m	$AAIII_{IDHmut}$	2234	balanced	no	120190000	$A2_{path}$	$A2_{CNVL}$	$A2_{combined}$
85	31	m	$AAIII_{IDHmut}$	1876	balanced	no	64692119	$A2_{path}$	$A2_{CNVL}$	$A2_{combined}$
86	35	m	$AAIII_{IDHmut}$	808	hetdel	no	47784811	$A2_{path}$	$A2_{CNVL}$	$A2_{combined}$
87	18	f	$AAIII_{IDHmut}$	2527	balanced	no	165846610	$A2_{path}$	$A2_{CNVL}$	$A2_{combined}$
88	20	m	$AAIII_{IDHmut}$	552	balanced	no	17370000	$A2_{path}$	$A2_{CNVL}$	$A2_{combined}$
89	41	m	$AAIII_{IDHmut}$	541	balanced	no	193578368	$A2_{path}$	$A2_{CNVL}$	$A2_{combined}$

90	60	m	$AAIII_{IDHmut}$	1116	balanced	no	206039846	$A2_{path}$	$A2_{CNVL}$	$A2_{combined}$
91	34	m	$AAIII_{IDHmut}$	1112	balanced	no	138650339	$A2_{path}$	$A2_{CNVL}$	$A2_{combined}$
92	32	f	$AAIII_{IDHmut}$	189	balanced	no	249098921	$A2_{path}$	$A2_{CNVL}$	$A2_{combined}$
93	34	m	$AAIII_{IDHmut}$	4403	balanced	no	349695798	$A2_{path}$	$A2_{CNVL}$	$A2_{combined}$
94	31	m	$AAIII_{IDHmut}$	8152	hetdel	no	84825223	$A2_{path}$	$A2_{CNVL}$	$A2_{combined}$
95	27	f	$AAIII_{IDHmut}$	2351	balanced	no	1852897	$A2_{path}$	$A2_{CNVL}$	$A2_{combined}$
96	27	m	$AAIII_{IDHmut}$	86	balanced	no	100983650	$A2_{path}$	$A2_{CNVL}$	$A2_{combined}$
97	39	f	$AAIII_{IDHmut}$	2049	balanced	no	498665062	$A2_{path}$	$A3_{CNVL}$	$A3_{combined}$
98	56	m	$AAIII_{IDHmut}$	253	hetdel	no	636279064	$A2_{path}$	$A3_{CNVL}$	$A3_{combined}$
99	44	f	$AAIII_{IDHmut}$	5464	balanced	no	760800250	$A2_{path}$	$A3_{CNVL}$	$A3_{combined}$
100	45	f	$AAIII_{IDHmut}$	1581	balanced	no	423820854	$A2_{path}$	$A3_{CNVL}$	$A3_{combined}$
101	32	f	$AAIII_{IDHmut}$	1145	hetdel	no	453251583	$A2_{path}$	$A3_{CNVL}$	$A3_{combined}$
102	38	m	$AAIII_{IDHmut}$	622	balanced	no	689926530	$A2_{path}$	$A3_{CNVL}$	$A3_{combined}$
103	46	f	$AAIII_{IDHmut}$	793	hetdel	no	434218283	$A2_{path}$	$A3_{CNVL}$	$A3_{combined}$
104	49	m	$AAIII_{IDHmut}$	748	hetdel	no	365496202	$A2_{path}$	$A3_{CNVL}$	$A3_{combined}$
105	53	m	$AAIII_{IDHmut}$	269	balanced	no	728398267	$A2_{path}$	$A3_{CNVL}$	$A3_{combined}$
106	30	m	$AAIII_{IDHmut}$	2436	balanced	no	363383060	$A2_{path}$	$A3_{CNVL}$	$A3_{combined}$
107	36	m	$AAIII_{IDHmut}$	289	hetdel	no	380840728	$A2_{path}$	$A3_{CNVL}$	$A3_{combined}$
108	48	f	$AAIII_{IDHmut}$	1349	balanced	no	510647250	$A2_{path}$	$A3_{CNVL}$	$A3_{combined}$
109	30	m	$AAIII_{IDHmut}$	1754	balanced	no	499800655	$A2_{path}$	$A3_{CNVL}$	$A3_{combined}$
110	33	m	$AAIII_{IDHmut}$	476	balanced	no	440645896	$A2_{path}$	$A3_{CNVL}$	$A3_{combined}$
111	50	f	$AAIII_{IDHmut}$	2817	balanced	no	358770474	$A2_{path}$	$A3_{CNVL}$	$A3_{combined}$
112	36	f	$AAIII_{IDHmut}$	7	gain	no	517861229	$A2_{path}$	$A3_{CNVL}$	$A3_{combined}$
113	48	f	$AAIII_{IDHmut}$	1898	hetdel	no	758714830	$A2_{path}$	$A3_{CNVL}$	$A3_{combined}$
114	33	m	$AAIII_{IDHmut}$	2436	balanced	no	468801667	$A2_{path}$	$A3_{CNVL}$	$A3_{combined}$
115	25	m	$AAIII_{IDHmut}$	3467	balanced	no	624356552	$A2_{path}$	$A3_{CNVL}$	$A3_{combined}$
116	30	f	$AAIII_{IDHmut}$	186	balanced	no	352744994	$A2_{path}$	$A3_{CNVL}$	$A3_{combined}$
117	36	m	$AAIII_{IDHmut}$	1830	balanced	no	618297540	$A2_{path}$	$A3_{CNVL}$	$A3_{combined}$
118	52	m	$AAIII_{IDHmut}$	849	hetdel	no	639333382	$A2_{path}$	$A3_{CNVL}$	$A3_{combined}$
119	53	m	$AAIII_{IDHmut}$	3625	balanced	no	1062531615	$A2_{path}$	$A3_{CNVL}$	$A3_{combined}$
120	46	m	$AAIII_{IDHmut}$	2863	hetdel	no	454173599	$A2_{path}$	$A3_{CNVL}$	$A3_{combined}$
121	46	m	$AAIII_{IDHmut}$	2183	hetdel	no	1315154012	$A2_{path}$	$A3_{CNVL}$	$A3_{combined}$
122	44	f	$AAIII_{IDHmut}$	961	balanced	no	673356226	$A2_{path}$	$A3_{CNVL}$	$A3_{combined}$
123		m	$AAIII_{IDHmut}$	2304	balanced	no	484685201	$A2_{path}$	$A3_{CNVL}$	$A3_{combined}$
124	41	f	$AAIII_{IDHmut}$	1442	balanced	no	911535916	$A2_{path}$	$A3_{CNVL}$	$A3_{combined}$
125	30	m	$AAIII_{IDHmut}$	1589	balanced	no	1190727105	$A2_{path}$	$A3_{CNVL}$	$A3_{combined}$
126	58	m	$AAIII_{IDHmut}$	1804	hetdel	no	900853650	$A2_{path}$	$A3_{CNVL}$	$A3_{combined}$
127	46	m	$AAIII_{IDHmut}$	61	balanced	no	474539606	$A2_{path}$	$A3_{CNVL}$	$A3_{combined}$
128	37	m	$AAIII_{IDHmut}$	4598	hetdel	no	552397505	$A2_{path}$	$A3_{CNVL}$	$A3_{combined}$
129	66	f	$AAIII_{IDHmut}$	787	balanced	no	1069350769	$A2_{path}$	$A3_{CNVL}$	$A3_{combined}$
130	37	f	$AAIII_{IDHmut}$	363	homodel	no	465715427	A4	A4	A4
131	36	f	$AAIII_{IDHmut}$	1024	homodel	no	831929597	A4	A4	A4
132	55	m	$AAIII_{IDHmut}$	581	homodel	no	930444025	A4	A4	A4
133	27	m	$AAIII_{IDHmut}$	2315	homodel	no	223793927	A4	A4	A4
134	28	m	$AAIII_{IDHmut}$	535	homodel	no	296028886	A4	A4	A4

135	68	m	$AAIII_{IDHmut}$	1198	homodel	no	866989174	A4	A4	A4
136	56	m	$AAIII_{IDHmut}$	879	homodel	no	1312842881	A4	A4	A4
137	40	m	$AAIII_{IDHmut}$	677	homodel	no	989539476	A4	A4	A4
138	49	f	$AAIII_{IDHmut}$	360	homodel	no	1142771330	A4	A4	A4
139	31	m	$AAIII_{IDHmut}$	1680	homodel	no	684135301	A4	A4	A4
140	57	m	$AAIII_{IDHmut}$	2184	homodel	no	644588335	A4	A4	A4
141	42	m	$AAIII_{IDHmut}$	985	homodel	no	1137070451	A4	A4	A4
142	58	m	$AAIII_{IDHmut}$	499	homodel	no	1304553626	A4	A4	A4
143		m	$AAIII_{IDHmut}$	1936	homodel	no	222558442	A4	A4	A4
144	25	f	$AAIII_{IDHmut}$	880	homodel	no	482618213	A4	A4	A4
145	36	m	GBM_{IDHmut}	302	balanced	present	0	$A3_{path}$	$A2_{CNVL}$	$A3_{combined}$
146	38	m	GBM_{IDHmut}	1293	hetdel	present	193419378	$A3_{path}$	$A2_{CNVL}$	$A3_{combined}$
147	50	m	GBM_{IDHmut}	1070	hetdel	present	347889943	$A3_{path}$	$A2_{CNVL}$	$A3_{combined}$
148	47	m	GBM_{IDHmut}	1063	balanced	present	201362719	$A3_{path}$	$A2_{CNVL}$	$A3_{combined}$
149	33	m	GBM_{IDHmut}	1740	hetdel	present	274299199	$A3_{path}$	$A2_{CNVL}$	$A3_{combined}$
150	34	m	GBM_{IDHmut}	3732	balanced	present	324522740	$A3_{path}$	$A2_{CNVL}$	$A3_{combined}$
151	45	f	GBM_{IDHmut}	3102	balanced	present	330020454	$A3_{path}$	$A2_{CNVL}$	$A3_{combined}$
152	15	m	GBM_{IDHmut}	1309	hetdel	present	458136707	$A3_{path}$	$A3_{CNVL}$	$A3_{combined}$
153	41	m	GBM_{IDHmut}	1890	balanced	present	1115095398	$A3_{path}$	$A3_{CNVL}$	$A3_{combined}$
154	38	m	GBM_{IDHmut}	1513	balanced	present	545004153	$A3_{path}$	$A3_{CNVL}$	$A3_{combined}$
155	45	f	GBM_{IDHmut}	405	hetdel	present	1590206155	$A3_{path}$	$A3_{CNVL}$	$A3_{combined}$
156	43	m	GBM_{IDHmut}	626	balanced	present	618971955	$A3_{path}$	$A3_{CNVL}$	$A3_{combined}$
157	33	f	GBM_{IDHmut}	1505	hetdel	present	941539384	$A3_{path}$	$A3_{CNVL}$	$A3_{combined}$
158		m	GBM_{IDHmut}	1313	hetdel	present	478025436	$A3_{path}$	$A3_{CNVL}$	$A3_{combined}$
159	27	m	GBM_{IDHmut}	765	balanced	present	414171054	$A3_{path}$	$A3_{CNVL}$	$A3_{combined}$
160	35	f	GBM_{IDHmut}	665	balanced	present	2059818464	$A3_{path}$	$A3_{CNVL}$	$A3_{combined}$
161	37	f	GBM_{IDHmut}	174	hetdel	present	358097638	$A3_{path}$	$A3_{CNVL}$	$A3_{combined}$
162	44	f	GBM_{IDHmut}	917	hetdel	present	593099167	$A3_{path}$	$A3_{CNVL}$	$A3_{combined}$
163	53	m	GBM_{IDHmut}	3544	balanced	present	1136518981	$A3_{path}$	$A3_{CNVL}$	$A3_{combined}$
164	38	m	GBM_{IDHmut}	690	hetdel	present	549311866	$A3_{path}$	$A3_{CNVL}$	$A3_{combined}$
165	23	m	GBM_{IDHmut}	480	balanced	present	569558376	$A3_{path}$	$A3_{CNVL}$	$A3_{combined}$
166	51	m	GBM_{IDHmut}	330	hetdel	present	903932607	$A3_{path}$	$A3_{CNVL}$	$A3_{combined}$
167	33	m	GBM_{IDHmut}	1710	balanced	present	485848840	$A3_{path}$	$A3_{CNVL}$	$A3_{combined}$
168	38	f	GBM_{IDHmut}	3540	balanced	present	707394101	$A3_{path}$	$A3_{CNVL}$	$A3_{combined}$
169	33	f	GBM_{IDHmut}	1860	hetdel	present	570848619	$A3_{path}$	$A3_{CNVL}$	$A3_{combined}$
170	35	m	GBM_{IDHmut}	390	hetdel	present	643888537	$A3_{path}$	$A3_{CNVL}$	$A3_{combined}$
171	23	m	GBM_{IDHmut}	1620	balanced	present	451313723	$A3_{path}$	$A3_{CNVL}$	$A3_{combined}$
172	47	f	GBM_{IDHmut}	1740	balanced	present	407272041	$A3_{path}$	$A3_{CNVL}$	$A3_{combined}$
173	41	m	GBM_{IDHmut}	1830	balanced	present	369144405	$A3_{path}$	$A3_{CNVL}$	$A3_{combined}$
174	49	m	GBM_{IDHmut}	1020	balanced	present	900834346	$A3_{path}$	$A3_{CNVL}$	$A3_{combined}$
175		m	GBM_{IDHmut}	360	balanced	present	1054050774	$A3_{path}$	$A3_{CNVL}$	$A3_{combined}$
176	26	m	GBM_{IDHmut}	1920	hetdel	present	471542557	$A3_{path}$	$A3_{CNVL}$	$A3_{combined}$
177	25	m	GBM_{IDHmut}	2940	balanced	present	511679183	$A3_{path}$	$A3_{CNVL}$	$A3_{combined}$
178	47	f	GBM_{IDHmut}	750	balanced	present	781997801	$A3_{path}$	$A3_{CNVL}$	$A3_{combined}$
179	43	f	GBM_{IDHmut}	360	balanced	present	1185670713	$A3_{path}$	$A3_{CNVL}$	$A3_{combined}$

180	31	f	GBM_{IDHmut}	1800	hetdel	present	455864908	$A3_{path}$	$A3_{CNVL}$	$A3_{combined}$
181	37	f	GBM_{IDHmut}	2040	balanced	present	555554816	$A3_{path}$	$A3_{CNVL}$	$A3_{combined}$
182	18	m	GBM_{IDHmut}	630	balanced	present	572076605	$A3_{path}$	$A3_{CNVL}$	$A3_{combined}$
183	32	m	GBM_{IDHmut}	632	balanced	present	422428971	$A3_{path}$	$A3_{CNVL}$	$A3_{combined}$
184	22	m	GBM_{IDHmut}	934	balanced	present	766615685	$A3_{path}$	$A3_{CNVL}$	$A3_{combined}$
185	27	f	GBM_{IDHmut}	1582	balanced	present	828095041	$A3_{path}$	$A3_{CNVL}$	$A3_{combined}$
186	38	m	GBM_{IDHmut}	360	balanced	present	1544228140	$A3_{path}$	$A3_{CNVL}$	$A3_{combined}$
187	21	f	GBM_{IDHmut}	2413	balanced	present	425183946	$A3_{path}$	$A3_{CNVL}$	$A3_{combined}$
188	31	m	GBM_{IDHmut}	734	hetdel	present	847090386	$A3_{path}$	$A3_{CNVL}$	$A3_{combined}$
189	60	m	GBM_{IDHmut}	297	homodel	present	807768413	A4	A4	A4
190	41	m	GBM_{IDHmut}	1107	homodel	present	495740703	A4	A4	A4
191	32	m	GBM_{IDHmut}	676	homodel	present	378012012	A4	A4	A4
192	45	f	GBM_{IDHmut}	559	homodel	present	659510395	A4	A4	A4
193	38	m	GBM_{IDHmut}	763	homodel	present	421896525	A4	A4	A4
194	30	f	GBM_{IDHmut}	612	homodel	present	774198635	A4	A4	A4
195	52	m	GBM_{IDHmut}	744	homodel	present	1007202573	A4	A4	A4
196	52	m	GBM_{IDHmut}	355	homodel	present	432740127	A4	A4	A4
197	47	m	GBM_{IDHmut}	420	homodel	present	354295141	A4	A4	A4
198	37	m	GBM_{IDHmut}	1740	homodel	present	673228823	A4	A4	A4
199	32	m	GBM_{IDHmut}	1440	homodel	present	713800664	A4	A4	A4
200	30	f	GBM_{IDHmut}	1860	homodel	present	409762641	A4	A4	A4
201	42	f	GBM_{IDHmut}	510	homodel	present	558904598	A4	A4	A4
202		f	GBM_{IDHmut}	1110	homodel	present	1026408664	A4	A4	A4
203	32	m	GBM_{IDHmut}	1020	homodel	present	428821854	A4	A4	A4
204	33	m	GBM_{IDHmut}	630	homodel	present	889020134	A4	A4	A4
205	29	f	GBM_{IDHmut}	360	homodel	present	313871779	A4	A4	A4
206	48	m	GBM_{IDHmut}	840	homodel	present	2420702864	A4	A4	A4
207	28	f	GBM_{IDHmut}	660	homodel	present	616412044	A4	A4	A4
208	32	m	GBM_{IDHmut}	1080	homodel	present	265982563	A4	A4	A4
209	27	m	GBM_{IDHmut}	13	homodel	present	873352072	A4	A4	A4
210	25	m	GBM_{IDHmut}	388	homodel	present	960004694	A4	A4	A4
211	56	m	GBM_{IDHmut}	1605	homodel	present	919954069	A4	A4	A4

Table 3

Diffuse astrocytic tumours

Diffuse astrocytic glioma, IDH-mutant, CDKN2A/B-intact, WHO grade II
Diffuse astrocytic glioma, IDH-mutant, CDKN2A/B-intact with necrosis, WHO grade III
Diffuse astrocytic glioma, IDH-mutant, CDKN2A/B-deleted, WHO grade IV

Table 1

parameter	min	max	split	n	rate	p-value
age (years)	15	70	54	190	< 54; 92%	< 0.05
gender male	0	1	na	130	m; 62%	0.01
cell count (n/mm^2)	734	9143	4604	130	< 4604; 62%	< 0.002
Ki67 (%)	0	97	14.5	144	< 14.5; 71%	< 0.01
pHH3 count (n/10HPF)	0	327	no split			
microvessel density (%)	0,2	8,7	1.2	82	>1.2; 39%	< 0.05
necrosis absent	0	1	na	144	present; 32%	<0.000005
vascular proliferation absent	0	1	na	129	absent; 61%	<0.001

Table 2

gene	alteration	n	p-value
CCND1	amplification (cutoff 0.35)	1	0.17
CCND2	amplification (cutoff 0.35)	27	0.15
CDK4	amplification (cutoff 0.35)	18	0.11
CDK6	amplification (cutoff 0.35)	6	0.13
CDKN2A/*B*	homo del (cutoff -0.415)	38	0.0001
EGFR	amplification (cutoff 0.35)	4	0.38
MDM4	amplification (cutoff 0.35)	5	0.09
MET	amplification (cutoff 0.35)	11	0.39
MYC	amplification (cutoff 0.35)	13	0.89
MYCN	amplification (cutoff 0.35)	12	0.001
NF1	homo del (cutoff -0.415)	4	0.52
NF2	homo del (cutoff -0.415)	4	0.32
PDGFRA	amplification (cutoff 0.35)	13	0.03
PPM1D	amplification (cutoff 0.35)	1	0.70
PTEN	homo del (cutoff -0.415)	3	0.11
RB1	homo del (cutoff -0.415)	12	0.001
SMARCB1	homo del (cutoff -0.415)	2	0.26

homo del = homozygous deletion